Manuscript #200710028

Telomere dysfunction and cell survival: Roles for distinct TIN2-containing complexes

Sahn-ho Kim[1,2]*, Albert R. Davalos[1], Seok-Jin Heo[1], Francis Rodier[1], Ying Zou[1], Christian Beausejour[1,3], Patrick Kaminker[4,5] , Steven M. Yannone[1] & Judith Campisi[1,4]

[1]Lawrence Berkeley National Laboratory, Life Sciences Division, 1 Cyclotron Road, Berkeley, California 94720 USA

[2]Present address: Vattikuti Urology Institute, Henry Ford Health System, 1 Ford Place, 2D36, Detroit, MI 48202 USA

[3]Present address: Département de Pharmacologie Centre de Recherche, CHU Ste-Justine, 3175 Côte Ste-Catherine, Montréal, Qc, H3T 1C5

[4]Buck Institute for Age Research, 8001 Redwood Blvd., Novato, California 94945 USA

[5]Present address: Human Genome Sciences, 14200 Shady Grove Rd. Rockville, MD, 20850 USA

*Correspondence: Sahn-Ho Kim, Vattikuti Urology Institute, Henry Ford Health System, 1 Ford Place, 2D36, Detroit, MI 48202
Telephone: 313-874-3249; Fax: 313-874-4324; Email: skim3@hfhs.org

Keywords: Apoptosis/Senescence/DNA damage/Telomere complexes

Running Title: Telomere complexes and cell survival.

Numbers of character: 39,068

Abstract

Telomeres are maintained by three DNA binding proteins (TRF1, TRF2 and POT1), and several associated factors. One factor, TIN2, binds TRF1 and TRF2 directly and POT1 indirectly. Along with two other proteins, TPP1 and hRap1, these form a soluble complex that may be the core telomere maintenance complex. It is not clear whether sub-complexes also exist *in vivo*. We provide evidence for two TIN2 sub-complexes with distinct functions in human cells. We isolated these two TIN2 sub-complexes from nuclear lysates of unperturbed cells and cells expressing TIN2 mutants TIN2-13, TIN2-15C, which cannot bind TRF2 or TRF1, respectively. In cells with wild-type p53 function, TIN2-15C was more potent than TIN2-13 in causing telomere uncapping and eventual growth arrest. In cells lacking p53 function, TIN2-15C was more potent than TIN2-13 in causing telomere dysfunction and cell death. Our findings suggest that distinct TIN2 complexes exist, and that TIN2-15C-sensitive subcomplexes are particularly important for cell survival in the absence of functional p53.

Introduction

Telomeres are the repetitive DNA sequence and specialized proteins that cap the ends of linear eukaryotic chromosomes and protect them from degradation or fusion by DNA repair processes. Telomere integrity and length maintenance are essential for prolonged cell proliferation and are thought to play important roles in suppressing aging and cancer (Blackburn, 2000; Rodier et al., 2005).

Telomere length is generally maintained by telomerase, a reverse transcriptase that adds telomeric DNA repeats to chromosome ends. Telomere length homeostasis also depends on proteins that act at telomeres in *cis* to control the recruitment or access of telomerase (Smogorzewska and de Lange, 2004). Most human cells do not express telomerase. Because DNA replication machineries cannot fully copy DNA 3' ends, such cells lose telomeric DNA with each S phase. When telomeres become critically short, the cells enter a permanent growth arrested state termed senescence (Rodier et al., 2005). Both telomerase-expressing and telomerase-negative cells utilize a host of proteins to ensure a proper protective telomeric structure.

The precise structure of mammalian telomeres is not known. However, a 't-loop' structure, in which the 3' overhang loops back and invades the telomeric DNA duplex, has been inferred by electron microscopy and biochemical experiments (Griffith et al., 1999). The t-loop model explains how telomeric ends are protected from recognition by DNA repair machineries. This protection is sometimes termed capping. Telomeres can become uncapped when critically short, presumably too short to form a t-loop, or when certain telomeric proteins are defective.

Several telomere-associated proteins are known to be important for telomere length regulation and capping (Rodier et al., 2005; Smogorzewska and de Lange, 2004). These include the direct telomeric DNA binding proteins TRF1, TRF2, and POT1, proteins that associate with these telomeric DNA binding

actors (e.g., TIN2, hRap1, tankyrases), and a variety of proteins involved in other processes, such as DNA repair and recombination. Of the direct DNA binding proteins, TRF1 binds double-stranded telomeric DNA and is an important regulator of telomere length (van Steensel and de Lange, 1997). In contrast, TRF2, which also binds double-stranded telomeric DNA, is more important for telomere capping (Karlseder et al., 1999; Smogorzewska and De Lange, 2002; van Steensel et al., 1998). POT1 binds the single-stranded 3' overhang and is likely a terminal regulator of telomere length and end protection (Baumann and Cech, 2001).

TIN2 is an important telomere-associated protein because it binds both TRF1 (Kim et al., 1999) and TRF2 (Kim et al., 2004; Liu et al., 2004a; Ye et al., 2004a) and indirectly interacts with POT1 via the intermediary protein TPP1 (also termed pTOP (Liu et al., 2004b), PIP1 (Ye et al., 2004b), and TINT1 (Houghtaling et al., 2004)). TIN2 participates in the regulation of telomere length through its interactions with TRF1 (Kim et al., 1999) and TPP1 (Houghtaling et al., 2004; Liu et al., 2004b; Ye et al., 2004b). In addition, TIN2 appears to be a critical component in forming telomere complexes that function in end-protection (Kim et al., 2004).

The functions of the three telomeric DNA binding proteins (TRF1, TRF2 and POT1) are very likely coordinated. Perturbations to either TRF1 or TRF2, or their associated proteins POT1, hRap1 or TIN2, influence both telomere length and capping (Iwano et al., 2004; Kim et al., 2004; Kim et al., 1999; Loayza and De Lange, 2003; van Steensel and de Lange, 1997; Yang et al., 2005). These observations suggest that TRF1, TRF2, POT1, and TIN2 may function in the same pathway. Consistent with this idea, six proteins co-purified in a large molecular weight complex (Liu et al., 2004a; O'Connor M et al., 2006; Ye et al., 2004a). This complex may be the core molecular machinery that regulates mammalian telomeres. On the other hand, gel filtration identified a TRF2-hRap1 complex that also contains TIN2 and POT1 but not TRF1 (Ye et al., 2004a).

Further, when TRF1 is removed from telomeres, TIN2 and TPP1 remain at telomeres via increased association with TRF2 (Houghtaling et al., 2004). And, although POT1 was shown to be associated with TRF1 (Loayza and De Lange, 2003), POT1 and TRF2 also form a complex with telomeric DNA, and POT1 overexpression protects against loss of telomeric single-stranded DNA caused by expression of a dominant negative TRF2 (DN-TRF2) (Yang et al., 2005). Thus, there may be distinct telomeric complexes that participate in maintaining telomere length and capping.

It is not yet clear whether there is a single TIN2 complex, which always contains TRF1, TRF2 and TPP1/POT1 and their interacting proteins, or whether TIN2 forms multiple complexes, some of which contain TRF1, while others contain TRF2 (Houghtaling et al., 2004; Kim et al., 2004; Ye et al., 2004a). Further, although it is hypothesized that telomeric complexes respond to telomere shortening, it is not known which telomere complexes are important for telomere capping, cellular senescence and cell death. Here, we report that at least two major TIN2-complexes can be identified by immunoprecipitation and gel-filtration of cell lysates, and that one of these is crucial for cellular senescence and cell survival in the absence of p53.

Results

TIN2 depletion disrupts TRF1 and TRF2 and causes cell death in the absence of p53 function

To understand the effects of TIN2 on cell fate and telomeric complex integrity, we used RNA interference (RNAi) to ablate TIN2 expression. We expressed short hairpin (sh) RNAs (Brummelkamp et al., 2002) complementary to three regions of the TIN2 mRNA (T2i-1, T2i-2, and T2i-3) in HT1080 human fibrosarcoma cells. Two of the shRNAs, T2i-2 and T2i-3, reduced TIN2 protein levels by 70-80% (Fig. 1a). T2i-2 and T2i-3 (not shown) also reduced TRF1 and TRF2 protein levels (Fig. 1b), consistent with the reported degradation of TRF1 upon removal from telomeres (Chang et al., 2003).

T2i-2 also reduced focal immunostaining, indicative of telomeric localization, of TIN2, TRF1, and TRF2 (Supplementary Fig. 1). Thus, loss of TIN2 completely disrupted telomeres, as determined by loss of TRF1 and TRF2 protein levels and telomeric occupancy.

Following the loss of telomeric TIN2, TRF1 and TRF2, T2i-2 and T2i-3 induced caspase-dependent cell death, indicative of apoptosis (Fig. 1c). Cell death was not observed when cells expressed an insertless vector, a non-specific (N/S) shRNA or T2i-1, which did not reduce TIN2 expression (Figs. 1a, c). T2i-2 also induced apoptosis in primary human fibroblasts (strains HCA2 and WI-38) (Fig. 1d). Strikingly, inactivation of p53 by GSE-22, a short peptide that disrupts p53 tetramerization and causes accumulation of monomeric p53 in these cells (Gudkov et al., 1993), failed to rescue WI-38 cells from T2i-2-induced apoptosis (Fig. 1d). Loss of p53 activity was confirmed by the absence of detectable p21 immunostaining and enhanced p53 immunostaining in X-irradiated GSE-22-expressing, but not control, cells (Fig. 1e). Thus, TIN2 was essential for TRF1 and TRF2 stability and occupancy at telomeres, as well as the viability of normal and tumor-derived human cells, regardless of p53 status. This result suggests that loss of TIN2 promotes a seriously aberrant telomeric structure that induces cell death, even in the absence of p53, similar to the effects of telomere disruption caused by expression of a mutant telomerase template RNA (Li et al., 2004).

TIN2-subcomplexes are formed in cells

To gain insight into physiologically relevant TIN2 complexes, we prepared nuclear extracts from HeLa cells using a modified Dignam protocol (Dignam et al., 1983). The majority of endogenous TRF1 is extracted by this high salt (>0.3 M KCl) method (Okabe et al., 2004). To detect TIN2 complexes, the extracts were dialyzed into buffer approximating physiological ionic strength and then fractionated by size-exclusion chromatography. The resulting fractions were

analyzed by western blotting (Figs. 2a, 2b).

We detected TIN2 across a broad range of molecular mass, from ≤1.5 MDa to ~100 kDa in fractions 13-33 (Fig. 2a). TRF1 eluted in two distinct peaks, co-eluting with TIN2 in fractions 15-17 and fractions 27-33. All six telomere-associated proteins (TRF1, TIN2, TRF2, hRap1, POT1, and TPP1) co-fractionated in fractions 15-17, consistent with the large complex termed shelterin (de Lange, 2005) and referred to here as complex C. We also observed a protein complex containing TIN2, TRF2, hRap1, POT1 and TPP1, but lacking TRF1 (Fig. 2a, fractions 19-23), consistent with previous reports (O'Connor et al., 2006; Ye et al., 2004a). We term this complex, complex B. The complex B we detected here differs somewhat from that previously reported (termed fraction 1, isolated by a two-step chromatographic protocol) (O'Connor et al., 2006), in which TPP1 was only marginally detectable. Our one step protocol, by contrast, showed that TPP1 was a prominent component of complex B. We quantified the signals from the western blots to illustrate the elution profiles of the six telomeric proteins (Fig. 2b).

Under our experimental conditions we observed an additional telomere protein complex (complex A) containing significant amounts of TIN2 and TRF1 in the lower molecular mass range (Fig. 2a, fractions 27-33). Fractions 27-31 also contained low levels of a TPP1/POT1 complex, as previously reported (Xin et al., 2007). However, in contrast to our findings (Fig. 2a), these studies (Liu et al., 2004a; O'Connor et al., 2006; Ye et al., 2004a) did not detect complex A in the same molecular mass range, possibly due to the lower salt used for extraction or different gel-filtration conditions. Complex A does not appear to arise from larger complexes (e.g., complex C) as a consequence of high salt extraction because there is no evidence of dissociated or degraded monomeric proteins (TRF2, POT1, TPP1, hRap1) in the low molecular weight fractions (Fig. 2a, fractions 35-49). This result is most consistent with a *bona fide* TRF1-TIN2 complex (complex A) existing *in vivo*. As expected, we detected degraded TIN2 in

fractions 57-65. We confirmed the absence of monomeric (and presence of degraded) proteins using twice the amount of sample and a different gel filtration column (Superdex S-200; 600-10 kDa that is better at fractionating low molecular weight proteins (Supplementary Fig. 2a). This fractionation showed that low molecular ranges (Supplementary Fig. 2a, fractions 29-55) contained only degradation products of TIN2 and TRF1. TRF1 is degraded when dissociated from telomeres (Chang et al., 2003). Moreover, the high salt nuclear extracts contained >90% of the TRF1, TRF2 and TIN2, suggesting that most of these proteins were released from telomeres (Supplementary Fig. 2b). These results suggest that complex A (TIN2-TRF1) might be degraded upon dissociation from telomeres by high salt (0.5 M); in lower salt (0.3 -0.4 M), this complex is not released from telomeres and therefore not detected.

Our chromatographic results are consistent with the existence of three heteromeric complexes (complexes A, B, and C), although, taken alone, the results are also consistent with each of the proteins being assembled into homomeric complexes of approximately equal size.

To discriminate between these possibilities and more directly probe telomeric protein assemblies without high salt extraction, we overexpressed epitope-tagged POT1, TIN2 or TRF1 (V5-tagged POT1, Flag-tagged TIN2, HA-tagged TRF1) in HT1080 cells. We prepared cell lysates using physiological ionic strength (0.15 M NaCl), which does not liberate endogenous TRF1 and TIN2 as determined by western blotting (not shown). We expected anti-V5 to immunoprecipitate complexes B and C, anti-HA to precipitate complexes A and C, and anti-Flag to precipitate all three complexes.

The major complex precipitated by HA antibodies (Fig. 2c lanes 10, 11) was complex A (TRF1-TIN2). A minor complex containing TRF1, TIN2 and TPP1 was also detectable. These findings suggest that most TRF1 proteins formed a complex with TIN2 under the immunoprecipitation conditions of RIPA

buffer and physiological salt.

V5-antibodies precipitated a major complex of POT1, TPP1,TIN2, TRF2 and hRap1 (complex B), regardless of whether TRF1 was overexpressed, and a minor complex containing TRF1,TIN2, TPP1, POT1,TRF2 and hRap1 (complex C). Because POT1 does not interact directly with TRF2 (Loayza and De Lange, 2003), this result suggests that POT1/TPP1 (Xin et al., 2007) forms a more stable complex with TIN2-TRF2/hRap1 than with TIN2-TRF1.

When Flag-TIN2 was the precipitating protein, Flag antibodies (Fig. 2c, lanes 6, 7) precipitated more complex B in the absence of overexpressed TRF1 than in its presence. This result suggests that TRF1 and TRF2 compete with TIN2 to form two separable complexes, A and B. In addition, we detected a small amount of complex C in lysates from cells that overexpressed TRF1 and TIN2. In the Discussion, we propose possible explanations for the relatively minor abundance of complex C after immunoprecipitation compared to nuclear extraction.

Together, the fractionation and immunoprecipitation data indicate the existence of distinct TIN2 complexes in cells. For simplicity, we term these complexes as follows: TRF1-TIN2, complex A; TIN2-TRF2/hRap1-TPP1/POT1, complex B; TRF1-TIN2-TRF2/hRap1-TPP1/POT1, complex C (Fig. 2d).

TIN2 mutants have distinct effects on TIN2-complexes.

TIN2-13 and TIN2-15C are TIN2 truncation mutants with different binding capabilities (Fig. 3a). TIN2-15C lacks TRF1 binding (Kim et al., 1999). It retains the TRF2 binding domain, but interacts less strongly than wild-type TIN2 with TRF2 (Kim et al., 2004). Immunoprecipitation of lysates from cells expressing epitope-tagged TIN2-15C and POT1 showed that TIN2-15C retains TPP1/POT1 binding (Fig. 3b). Reciprocally, TIN2-13 retains TRF1 binding (Kim et al., 1999), but lacks TRF2 (Kim et al., 2004) and TPP1/POT1 (Ye et al., 2004b) binding.

We used these mutants to identify TIN2 complexes in cells, and determine their role in the cell death caused by complete loss of TIN2 in p53-deficient cells.

We first tested the effects of TIN2 mutants on complex A, B and C formation. Based on their composition (Fig. 2), we predicted that TIN2-13, which lacks TPP1 and TRF2 binding (Liu et al., 2004b; Ye et al., 2004b), would perturb complexes A and C, whereas TIN2-15C, which lacks TRF1 binding, would perturb complexes B and C (Fig. 3a). We expressed V5-POT1 plus wild-type TIN2, TIN2-13 or TIN2-15C in HT1080 cells, and immunoprecipitated cell lysates using V5 antibodies (Fig. 3c, lanes 5-8).

When TIN2-13 was expressed, V5 antibodies did not precipitate TIN2-13, and the level of endogenous TIN2 was not altered in the precipitate (note anti-V5 precipitated less POT1 in Fig. 3c, lane 6, and compare lanes 6 and 7). This result indicates that V5-POT1 mainly precipitated TIN2 B complexes, and that TIN2-13 does not disrupt complex B, as predicted. This result also confirms the inability of TIN2-13 to interact with TRF2 (Kim et al., 2004) and TPP1/POT1 (Ye et al., 2004b).

By contrast, when TIN2-15C was expressed, V5 antibodies precipitated TIN2-15C, and the presence of TIN2-15C reduced the level of endogenous TIN2 in the precipitate (lane 8). Further, TIN2-15C expression reduced the level of TRF2 in the precipitate (Fig. 3c, compare lanes 6 and 8), indicating that TIN2-15C inhibits the TIN2-TRF2 interaction. This result suggests that TIN2-15C disrupts complex B formation, as predicted, and is consistent with the finding that TIN2-15C reduces TRF2 stability in cells and dissociates TRF2 from telomeres (Kim et al., 2004). TIN2-15C or DN-TRF2 slightly reduced (84% and 89%, respectively) the length of the 3'-single-stranded telomeric overhang in normal HCA2 cells (Supplementary Fig.3). Inactivation of TRF2 by DN-TRF2 or TRF2 deletion reduced or slightly increased the 3' overhang length in cells that were deficient in p53 or in both p53 and ligase IV (van Steensel et al., 1998) (Celli and

de Lange, 2005). Thus, TIN2-15C and DN-TRF2 may have similar effects on 3'-overhang length regulation in normal cells.

We also expressed HA-TRF1 plus wild-type TIN2, TIN2-13 or TIN2-15C, and immunoprecipitated lysates using HA antibodies (Fig. 3d, lanes 13-16). TIN2-13 reduced the binding of endogenous TIN2 to HA-TRF1 (compare lanes 13 and 15), but TIN2-15C did not disrupt this interaction (compare lanes 13 and 16). Thus, as predicted, TIN2-13 disrupted TIN2-TRF1 complexes (complex A), but TIN2-15C did not.

We conclude that the TIN2 mutants TIN2-13 and TIN2-15C disrupt different TIN2 complexes, at least by immunoprecipitation analysis, and thus favor the formation of different telomeric complexes when expressed in cells.

Effects of TIN2 mutants in cells

To determine the biological effects of the TIN2 complexes, we expressed GFP (control), TIN2-13 or TIN2-15C in primary human fibroblasts (strain HCA2). We also analyzed these cells after p53 inactivation, achieved by expressing GSE-22 (Gudkov et al., 1993) or a p53 short hairpin RNA (sh-p53).

We first tested presenescent (P) or replicatively senescent (S) cells, with or without p53 inactivation, and measured apoptotic cell death using a sensitive cumulative assay (Goldstein et al., 2005) (Fig. 4a). We define presenescent cultures as those that retain >70% of their replicative life span, and thus contain cells with mostly long, functional telomeres. In contrast to the robust cell death caused by complete loss of TIN2 (Fig. 1c, d), TIN2-13 or TIN2-15C caused little or no cell death when expressed in P or S cells with normal p53 function (Fig. 4a). However, when p53 was inactivated, the fraction of apoptotic cells increased in both cell populations (Fig. 4a). Notably, co-expression of TIN2-13 and GSE-22 elevated apoptosis only about 2-fold above the levels in control cells (expressing GFP and GSE-22), whereas co-expression of TIN2-15C and GSE-22 increased

cell death 8- to 10-fold above control levels (Fig. 4a). Co-expression of TIN2 mutants with sh-p53 gave very similar results (Fig. 4a). These findings suggest that disruption of the TIN2-TRF2 or TIN2-TPP1/POT1 interaction (by TIN2-15C) has more severe consequences for cell survival than disruption of the TIN2-TRF1 interaction (by TIN2-13). They also indicate that disruption of telomeric complexes B and C (by TIN2-15C) is more deleterious than disruption of complex A and C (by TIN2-13). Moreover, the cell death caused by disrupting these complexes does not require p53 function.

Late generation mice lacking both telomerase and p53 progress very few generations relative to telomerase deficiency alone, suggesting the existence of a telomere-dependent cell death pathway that does not require p53 (Chin et al., 1999). To further test the idea that disruption of different telomeric complexes differentially affects the survival of cells that lack p53 function, we used lentiviral vectors to express TIN2 mutants and GSE-22 in replicatively senescent HCA2 fibroblasts. These senescent cells have several short, dysfunctional telomeres (Zou et al., 2004), similar to those in late generation telomerase-deficient mice. Moreover, because HCA2 cells express low levels of p16 (not shown), which inhibits the proliferation of cells that lack p53 function, p53 inactivation causes senescent HCA2 cells to resume proliferation, as reported for other low p16-expressing human fibroblast strains (Beausejour et al., 2003). We measured the ability of senescent HCA2 cells to form colonies following p53 inactivation and disruption of telomere complexes by TIN2 mutants. We compared the effects of TIN2 mutants to the effect of DN-TRF2, which uncaps telomeres and induce p53-dependent cell death (Karlseder et al., 1999) (Fig. 4b).

Senescent cells readily formed colonies upon expression of GSE-22, as expected (Beausejour et al., 2003). Subsequent expression of GFP (control), TIN2-13, or DN-TRF2 had no effect on colony formation after 12 (Fig. 4b) or 30 (not shown) days. By contrast, subsequent expression of TIN2-15C initially had no effect on cell proliferation (for 3-10 days; not shown), but then dramatically

reduced colony formation. The differences between TIN2-15C and TIN2-13 or DN-TRF2 in supporting colony formation could not be explained by differences in protein expression levels because TIN2-13 and DN-TRF2 were expressed more robustly than TIN2-15C (Fig. 4c).

Together, these findings suggest that p53-dependent cell growth requires both TIN2 A and B complexes. By contrast, the growth of cells that lack p53 function does not require TIN2 A complexes, which are disrupted by TIN2-13 (Fig. 3), but does require TIN2 B complexes, which are disrupted by TIN2-15C (Fig. 3). DN-TRF2, which lacks the TRF2 DNA binding domain and causes p53-dependent cell death (Karlseder et al., 1999), is clearly not equivalent to TIN2-15C in biological activity, possibly because it does not affect POT1 function in complex B (see Discussion).

We confirmed the selective sensitivity of p53-deficient cells to TIN2-15C using several human cancer cell lines. These included HT1080 fibrosarcoma cells (which were reported to undergo no cell death upon expression of DN-TRF2 (Karlseder et al., 1999)), MDA-MB-231 and MDA-MB-157 breast cancer cells, and PPC-1 prostate cancer cells. We used a transfected pIRES2-eGFP vector (Kim et al., 2004) and measured apoptotic cell death. TIN2-15C expression induced significant cell death within 48 h in all these p53-deficient cancer cells (Fig. 4d), whereas TIN2-13 was 2- to 8-fold less effective, depending on the cell line (Fig. 4d). Compared to normal cells in which p53 was inactivated by GSE-22, apoptosis was more robust in the cancer cells, being evident as early as 18 h after transfection, presumably because cancer cells harbor multiple mutations that disrupt cell growth and survival pathways. The TIN2 mutants caused much less cell death in p53-positive cancer cells (MCF-7; LN-Cap) (Fig. 4d). In all cases, TIN2-15C, but to a lesser extent TIN2-13, caused substantial cell death in p53-deficient cells (Fig. 4d), but very little cell death in cells with wild-type p53 (Fig. 4a).

Normal cells responded to TIN2-15C by undergoing senescence. TIN2-15C,

much more than TIN2-13, retarded cell proliferation (Fig. 5a) and induced senescence-associated-β-galactosidase (Fig. 5b). Both mutants also induced 53BP1/γH2AX foci (d'Adda di Fagagna et al., 2003; Takai et al., 2003). Most of these foci (60%-90%) co-localized with a telomeric DNA probe (Supplementary Figure 4), indicating that they marked dysfunctional telomeres. The TIN2 mutants induced 53BP1 foci in presenescent cells as well as replicatively senescent cells, which already have several telomeric 53BP1 foci. In all cases, TIN2-15C induced many more 53BP1 foci than TIN2-13 (Fig. 5c), suggesting that TIN2-15C is more potent than TIN2-13 at uncapping telomeres. These results also suggest that B complexes are more important than A complexes for protecting cells from cell death.

Chromosomal abnormalities induced by TIN2 mutants

Although p53-deficient cancer cells underwent rapid cell death in response to TIN2-15C, p53 inactivation and TIN2-15C expression did not cause rapid cell death in presenescent or senescent normal human fibroblasts (in contrast to the effect of TIN2 depletion). Thus, additional events, such as cell cycle progression, chromosome fusion and anaphase bridge formation, might be necessary for the death of cells with lesions that inactivate p53 and complex B. To test this idea, we expressed GFP (control), TIN2-13 or TIN2-15C in HCA2 cells in which p53 was inactivated by GSE-22. Cells expressing TIN2-15C had a significantly more chromosome fusions (0.85 per metaphase) and anaphase bridges or micronuclei (~21%), compared to cells expressing TIN2-13 (0.19 per metaphase, ~6% anaphase bridges/micronuclei) (Table 1; Supplementary Fig. 5). We observed no chromosome fusions and ~4% anaphase-bridges/micronuclei in cells expressing GFP. Fluorescence *in situ* hybridization with a telomeric probe showed that most of the fused chromosomes in TIN2-15C expressing cells possessed a telomeric signal (0.68 per metaphase), indicative of telomeric uncapping and subsequent fusion. These fusions are similar in type and level those reported for cells expressing DN-TRF2 (Hockemeyer et al., 2005; van Steensel et al., 1998; Yang et al., 2005), consistent with findings that TIN2 and

TRF2 interact and TIN2-15C reduces telomeric TRF2 (Kim et al., 2004). A small fraction of fusions lacked telomeric signal (0.16 per metaphase), which is more common upon loss of POT1 function (Wu et al., 2006). These results suggest that TIN2-15C may cause the death of p53-deficient cells indirectly by driving chromosome fusions and mitotic catastrophe.

Telomerase does not rescue TIN2-15C lethality

Telomerase can rescue senescent cells in which p53 has been inactivated from crisis caused by dysfunctional telomeres. To determine whether telomerase can similarly rescue p53-deficient senescent cells from the dysfunctional telomeres caused by TIN2-15C, we co-expressed the telomerase catalytic subunit (hTERT) and TIN2-15C in senescent HCA2 cells in which p53 was inactivated by GSE-22. Telomerase prevented the crisis that limits the proliferative capacity of these cells to ~20 population doublings (Beausejour et al., 2003). However, co-expression of telomerase and TIN2-15C did not rescue the cells from loss of proliferative potential (Fig. 6a, b). These results suggest that TIN2-15C causes cell death by disrupting telomeric structure and capping rather than by shortening telomere length.

Discussion

TIN2 telomeric complexes

Six telomere-associated proteins (TRF1-TIN2-TPP1-POT1-TRF2-hRAP1) have been isolated as a single soluble complex (Liu et al., 2004a; Ye et al., 2004a). TIN2 occupies a unique position in this complex because it interacts directly with TRF1 and TRF2, and indirectly (through TPP1) with POT1. In these studies, TRF2-complexes contained TIN2 and POT1, but not TRF1, suggesting that TRF1 is not required for the TRF2/hRap1-TIN2-TPP1/POT1 interaction (Houghtaling et al., 2004). TRF1 and TRF2 bind non-cooperatively along telomeric repeats and have high off-rates *in vitro* (Bianchi et al., 1999). These results suggest that TIN2 may form dynamic TRF1 or TRF2 complexes at

telomeres. We identified three major soluble TIN2 complexes (TRF1-TIN2, complex A; TIN2-TRF2/hRap1-TPP1/POT1, complex B; and TRF1-TIN2-TRF2/hRap1-TPP1/POT1, complex C) from nuclear extracts containing endogenously expressed proteins, supporting the idea that TRF1 and TRF2 complexes are separable.

Previously reports (Liu et al., 2004a; Ye et al., 2004a) did not detect complex A, suggesting our nuclear extraction protocol, which used higher salt concentrations, was more effective at dissociating TIN2-TRF1 complexes from telomeres or the nuclear matrix. TRF1 cross-reactivity was detected as multiple bands in low molecular weight fractions, which is likely due to proteolysis after release from telomeres (Chang et al., 2003) or the nuclear matrix (Okabe et al., 2004). In addition, we did not detect complex C as a major complex in cells that overexpressed TRF1 and TIN2 and were extracted by physiological salt. Complex C formation may require telomeric DNA, t-loop formation, and/or posttranslational modifications to TRF1 or matrix-associated TRF1.

We utilized two TIN2 mutants with distinct abilities to disrupt the major TIN2 complexes (A and B). TIN2-13 affected the TRF1-TIN2 complex A, whereas TIN2-15C affected TRF2-complexes. If the major telomeric complex were a single entity (complex C), TIN2-13 and TIN2-15C should disrupt this complex similarly. However, our results are more consistent with the existence of two separable TIN2 complexes, which may have different functions in cells.

TIN2 complexes may function differently.

In normal cells, telomeres shorten with each division, eventually causing senescence. TIN2-15C, which disrupts complex B, removes TRF2 from telomeres and induces DNA damage foci, but TRF1 remains at telomeres (Kim et al., 2004). DN-TRF2 also removes TRF2 and induces DNA damage foci containing TRF1 (Takai et al., 2003). Senescent cells with short telomeres and telomeric DNA damage foci frequently lack TRF2 but not TRF1 (Herbig et al.,

2004). Thus, short telomeres may preferentially attract A complexes, and senescent cells may be unable form enough complex B (TIN2-TRF2/hRap1-TPP1/POT1) because TIN2 is bound primarily in A (TRF1-TIN2) complexes. Alternatively, complexes A and B may have different preferred locations on the telomere or t-loop, and cooperate in telomere capping.

TRF1-TIN2 complexes stimulate interactions between telomeric DNA tracts *in vitro*, suggesting that this complex modulates a tertiary telomeric structure (Kim et al., 2003). TIN2-13, which disrupts this complex (complex A), may decrease the complexity of the telomeric structure. On the other hand, deletion of TRF2 or POT1 causes telomere uncapping and chromosome fusion, suggesting that complex B is essential for telomere end protection (Hockemeyer et al., 2006; Wu et al., 2006). Consistent with this view, we found that TIN2-15C, which disrupts complex B, uncapped telomeres and caused telomeric fusions and anaphase bridges. Thus, we favor the hypothesis that TRF1-TIN2 (A) complexes and TIN2-TRF2/hRap1-TPP1/POT1 (B) complexes have different locations at telomeres and cooperate to form the telomeric cap (Fig.6c). B complexes are more important for ensuring a proper terminal or t-loop structure, whereas A complexes modulate the telomeric tertiary structure and enhance the stability and function of complex B. Although TIN2-13 induces some telomere uncapping and telomeric fusion, the effects of TIN2-13 are less pronounced than those of TIN2-15C, suggesting that complex A supports the functions of complex B.

Alternatively, complexes A and B may cooperate to form the six protein complex C (also termed shelterin (de Lange, 2005)), and this complex may be the essential entity for telomere capping and cell survival. TIN2-13 may be less efficient than TIN2-15C at disrupting complex C. TPP1 may be an important regulator of complex C formation because loss of TPP1 can reduce the TRF1-TRF2-Rap1 interaction (O'Connor M et al., 2006).

Telomere-dependent cell survival in cells with or without p53 function

Late generation mice lacking both telomerase and p53 have a higher incidence of cancer relative to animals lacking only telomerase (Chin et al., 1999), implicating p53 as a key regulator of the response to telomere dysfunction. However, mice deficient in both p53 and telomerase lose sterility after only a few generations, indicating a second p53-independent block to cell viability (Chin et al., 1999). Expression of dominant-negative telomerase proteins (Hahn et al., 1999) or mutant telomerase RNAs (Guiducci et al., 2001) induces death in cells with either wild type or mutant p53, supporting the idea that loss of viability caused by telomere dysfunction is not dependent on a functional p53 response. By contrast, cell death or growth inhibition due to expression of DN-TRF2 is p53-dependent (Karlseder et al., 1999; Smogorzewska and De Lange, 2002).

Our results indicate that complex B disruption by TIN2-15C induce telomere dysfunction and cell cycle arrest in p53-positive cells. However, p53-deficient cells that express TIN2-15C continue to divide, developing chromosome-end fusions and anaphase bridges. These abnormalities result in cell death, which does not require p53 function. Thus, our findings support the idea that complex B disruption by TIN2-15C causes cell death which is independent of p53 due to severe genomic damage and mitotic catastrophe (Fig.6c). Our results also suggest that DN-TRF2 and TIN2-15C have different effects on the integrity of complex B.

In the absence of p53 activity, senescent cells that express little or no p16 can resume growth, although their proliferation is eventually limited by severe telomere shortening, crisis and cell death (Beausejour et al., 2003). Expression of telomerase eliminated this growth limitation. Expression of TIN2-13 and DN-TRF2 only minimally affected this growth resumption, whereas TIN2-15C expression accelerated this growth limitation. Recent findings (Hockemeyer et al., 2006; Hockemeyer et al., 2005; Wu et al., 2006) suggest an explanation for why the effects of TIN2-15C differ from those of DN-TRF2. Although, POT1 deficiency causes a telomere uncapping phenotype similar to that caused by TRF2 loss, POT1 and TRF2 likely have distinct functions in protecting telomeres, regulating nucleolytic processing, and controlling telomeric recombination. Thus,

TIN2-15C and DN-TRF2 likely inactivate TRF2 and POT1 differently in complex B. Since DN-TRF2 induces p53-dependent apoptosis (Karlseder et al., 1999), whereas TIN2-15C caused cell death in p53 deficient cells, our findings offer an explanation for why ablation of TIN2 in cells (Fig. 1) and in the mouse germ line (Chiang et al., 2004) causes cell lethality or senescence, regardless of p53 status.

It remains to be understood how telomere dysfunction causes cell death in p53 deficient cells, how dysfunctional telomeres are sensed as DNA damage, and the nature of the p53-dependent and p53-independent sensing mechanisms. Despite these gaps in our knowledge, telomerase inactivation has been proposed as an anti-cancer strategy because most cancer cells maintain telomere length by expressing this enzyme. Likewise, disruption of TIN2-complexes may provide a strategy for preferential killing of cancer cells, most of which lack p53 function. Thus, TIN2-15C sensitive complexes may provide a sensitive target for selective elimination of p53-deficient cancer cells.

Materials and Methods:

Cell culture, senescence and apoptosis characterization: We cultured all cells, and measured senescence-associated β-galactosidase, as described (Dimri et al., 1995). We determined cell death by collapse of the mitochondrial membrane potential (Davalos and Campisi, 2003) or by a cumulative assay in which cells are incubated with a caspase inhibitor for 3 days and scored for cytosolic cytochrome c (Goldstein et al., 2005).

Separation of native TIN2 complexes: Nuclei were isolated from HeLa-S3 cell suspension cultures (20 l; 1 X10^6 cells/ml) (National Cell Culture Center, Minneapolis), and extracted with KCl (0.5 M) by a modified nuclear extraction method (Dignam et al., 1983). Extracts were dialyzed into S-300 chromatography buffer (50 mM Tris pH 7.5, 150 mM KCl, 0.2mM EDTA, 20% glycerol, 0.025% NP-40, 0.5 mM dithiothreitol, 1 μg/ml aprotinin, pepstatin A and

leupeptin and 0.5 mM PMSF) and cleared by centrifugation at 15,000 rpm for 30 min at 4° C. The dialyzed sample (2. 5 ml) was loaded onto a Sephacryl S-300-HR (Pharmacia) column (1.6/60 cm, 125 ml) equilibrated with S-300 buffer. Fractions (1.4 ml) were collected and stored at 4° C. The S-300 column was calibrated using molecular mass standards (blue dextran, thyroglobulin, ferretin, aldolase, conalbumin) (GE healthcare) according to the manufacture's instructions.

We expressed FLAG-tagged TIN2 and HA-tagged TRF1 in HT1080 cells using the retroviral vector pLXSN, as described (Kim et al., 1999). V5-tagged POT1(Baumann et al., 2002) and myc-TIN2 mutants (TIN2-13 or TIN2-15C) were expressed using the pIRE2-EGFP vector (Bio Science) and transient transfection using Fugene 6 (Roche). Cells (6 x 10^6) were washed with phosphate buffered saline (PBS), and 1 ml RIPA buffer (50 mM Tris (pH 7.5), 150 mM NaCl, 1% NP-40, 1 mM EDTA, 10% glycerol, protease inhibitor cocktail) (Roche) was added to each plate. After incubation on ice for 30 min, cells were collected by scraping and centrifugation at 4° C, and the supernatant (cell lysate) was recovered.

Immunoprecipitation and western analyses: We incubated cell lysates (200-300 μg protein) with 2 μg HA antibody (Roche), 10 μg FLAG M2 antibody (Sigma) or 2 μg V5 antibody (Invitrogen) for 2 h at 4˚ C, and added 50 μl of a 50% protein G-Sepharose slurry (Invitrogen) for 2 h at 4˚ C. We washed the immune complexes with RIPA buffer and analyzed proteins by western blotting as described (Davalos and Campisi, 2003; Kim et al., 1999). Primary antibodies were monoclonal anti-TRF2 (IMG-124A, Imgenex), polyclonal anti-hRap1 (IMG-289, Imgenex), polyclonal anti-TRF1 (H-242, Santa Cruz; ab1423, Abcam), polyclonal anti-POT1 (H200, Santa Cruz), polyclonal anti-HA- or -TRF2 or monoclonal anti-HA (Santa Cruz), monoclonal anti-V5 (Invitrogen), polyclonal anti-TIN2 (Kim et al., 1999) and polyclonal TPP1 (O'Connor M et al., 2006).

Immunostaining: We immunostained cells as described (Kim et al., 1999). Briefly, we cultured cells in chamber slides, fixed with 4% formalin, permeabilized

with 0.5% Triton-X100, and stained with anti-TRF2, anti-TIN2 (Kim et al., 1999), polyclonal anti-53BP1 (Abcam), monoclonal anti-p21 (Pharmigen), monoclonal anti-p53 (Oncogene) or control (10% goat) serum (Vector). After washing, we stained with secondary antibodies conjugated to Texas Red or FITC (Molecular probes), and counterstained the nuclei with DAPI. Images of cells were acquired on a microscope (BX60; Olympus) using either a 100X UPlanFL 1.3 NA (Olympus) lens with oil or a 40X UPlanFL 0.5 NA (Olympus) lens without oil. Images were acquired with a CCD camera (Diagnostic Instruments Inc) and captured into SPOT imaging software (Diagnostic Instruments Inc). All the modifications were applied to the whole image using Canvas 8 (Deneba) or Photoshop CS (Adobe).

Chromosome analyses: Telomeres were visualized by *in situ* hybridization (FISH) on metaphase spreads using a telomeric protein nucleic acid (PNA) probe, as described (Hultdin et al., 1998). Cells treated with colcemid (0.1 μg/ml) for 4 h were trypsinized and collected at 1000 X *g* (5 min). After hypotonic swelling in 30 mM Na-citrate for 20 min at 37^{o} C, the cells were fixed in methanol:acetic acid (3:1). FISH, using a Cy3-labeled $(CCCTAA)_3$ PNA probe (Applied Biosystem), and scoring for telomeric fusions were performed as described (Bailey et al., 1999).

3'-G-rich strand overhangs were measured as described (Kim et al., 1999). 4 μg genomic DNA were hybridized with telomeric C-stranded probes $(CCCTAA)_5$ in non-denaturing buffer to detect the 3' overhang and in denaturing buffer to detect total telomeric DNA.

shRNA and expression vectors: Where indicated, cells were infected with a retrovirus expressing GSE-22 (Gudkov et al., 1993) or a lentivirus expressing sh-p53 (Nair et al., 2005), selected and then transfected with expression vectors or infected with lentiviruses, as described (Beausejour et al., 2003; Kim et al., 2004). To ablate TIN2 expression, we synthesized double stranded DNAs to target the TIN2 mRNA (T2i-1: caggtgaagcagctgtcag; T2i-2: ggtcatatctaatcctgag, T2i-3:

gtggtggtggagctgatc) or SATB1, a nuclear protein that is not expressed in fibroblasts or HT1080 cells (N/S, non-specific): aacagctactattgccact). We cloned the DNA into the pSuper vector (Brummelkamp et al., 2002), and transiently transfected packaging cells using FuGene6 (Roche). We cloned TIN2 mutants into the bicistronic pIRES2-EGFP (Clontech) or pPRL-Sin18-lenti vector(Dull et al., 1998). Lentiviruses were used at equivalent titers, sufficient to infect approximately 80-90% of cells.

Colony formation assay: Senescent cells (<2% labeling index) were plated with 5 x 10^4 cells in 6 well plates and infected with lentiviruses expressing GFP, TIN2-15C, TIN2-13, hTERT or GSE-22 as described (Beausejour et al., 2003). The cells were washed with PBS twice, fixed and stained with 0.1 % crystal violet in 10% ethanol for 5 min at room temperature, washed with PBS and dried.

Online supplemental material:

Supplementary Figure 1 shows that TIN2 reduction decreases TRF1 and TRF2 foci in immunostaining. Supplementary Figure 2 presents additional fractionation of TIN2-TRF1 complexes from HeLa cell nuclear lysate on a Superdex S-200 HR (Pharmacia) column, and shows that nuclear extraction efficiently liberates telomeric proteins in our extraction protocol. Supplementary Figure 3 presents telomeric G-strand overhangs and telomere length analyses in cells expressing TIN2-15C and DN-TRF2. Supplementary Figure 4 shows telomeric damage responses that are co-stained for telomeric DNA in cells expressing TIN2-13 or TIN2-15C. Supplementary Figure 5 shows telomeric fusions and anaphase-bridges in cells expressing TIN2-15C.

Acknowledgements:

We thank Zhou Songyang for TPP1 antibodies, Peter Baumann for the POT1-V5 cDNA and Yoichi Shinkai for critical reading of the manuscript. We acknowledge support from the National Institutes of Health and California Breast Cancer Research Program. This work was supported by the Director, Office of Science,

Office of Basic Energy Sciences, of the U.S. Department of Energy under Contract No. DE-AC02-05CH11231.

References:

Bailey, S.M., J. Meyne, D.J. Chen, A. Kurimasa, G.C. Li, B.E. Lehnert, and E.H. Goodwin. 1999. DNA double-strand break repair proteins are required to cap the ends of mammalian chromosomes. *Proc Natl Acad Sci U S A*. 96:14899-904.

Baumann, P., and T.R. Cech. 2001. Pot1, the putative telomere end-binding protein in fission yeast and humans. *Science*. 292:1171-5.

Baumann, P., E. Podell, and T.R. Cech. 2002. Human Pot1 (protection of telomeres) protein: cytolocalization, gene structure, and alternative splicing. *Mol Cell Biol*. 22:8079-87.

Beausejour, C.M., A. Krtolica, F. Galimi, M. Narita, S.W. Lowe, P. Yaswen, and J. Campisi. 2003. Reversal of human cellular senescence: roles of the p53 and p16 pathways. *Embo J*. 22:4212-22.

Bianchi, A., R.M. Stansel, L. Fairall, J.D. Griffith, D. Rhodes, and T. de Lange. 1999. TRF1 binds a bipartite telomeric site with extreme spatial flexibility. *Embo J*. 18:5735-44.

Blackburn, E.H. 2000. Telomere states and cell fates. *Nature*. 408:53-6.

Brummelkamp, T.R., R. Bernards, and R. Agami. 2002. A system for stable expression of short interfering RNAs in mammalian cells. *Science*. 296:550-3.

Celli, G.B., and T. de Lange. 2005. DNA processing is not required for ATM-mediated telomere damage response after TRF2 deletion. *Nat Cell Biol*. 7:712-8.

Chang, W., J.N. Dynek, and S. Smith. 2003. TRF1 is degraded by ubiquitin-mediated proteolysis after release from telomeres. *Genes Dev*. 17:1328-33.

Chiang, Y.J., S.H. Kim, L. Tessarollo, J. Campisi, and R.J. Hodes. 2004. Telomere-associated protein TIN2 is essential for early embryonic development through a telomerase-independent pathway. *Mol Cell Biol*. 24:6631-4.

Chin, L., S.E. Artandi, Q. Shen, A. Tam, S.L. Lee, G.J. Gottlieb, C.W. Greider, and R.A. DePinho. 1999. p53 deficiency rescues the adverse effects of telomere loss and cooperates with telomere dysfunction to accelerate carcinogenesis. *Cell*. 97:527-38.

d'Adda di Fagagna, F., P.M. Reaper, L. Clay-Farrace, H. Fiegler, P. Carr, T. Von Zglinicki, G. Saretzki, N.P. Carter, and S.P. Jackson. 2003. A DNA damage checkpoint response in telomere-initiated senescence. *Nature*. 426:194-8.

Davalos, A.R., and J. Campisi. 2003. Bloom syndrome cells undergo p53-dependent apoptosis and delayed assembly of BRCA1 and NBS1 repair complexes at stalled replication forks. *J Cell Biol*. 162:1197-209.

de Lange, T. 2005. Shelterin: the protein complex that shapes and safeguards human telomeres. *Genes Dev*. 19:2100-10.

Dignam, J.D., R.M. Lebovitz, and R.G. Roeder. 1983. Accurate transcription initiation by RNA polymerase II in a soluble extract from isolated mammalian nuclei. *Nucleic Acids Res*. 11:1475-89.

Dimri, G.P., X. Lee, G. Basile, M. Acosta, G. Scott, C. Roskelley, E.E. Medrano, M. Linskens, I. Rubelj, O. Pereira-Smith, and et al. 1995. A biomarker that identifies senescent human cells in culture and in aging skin in vivo. *Proc Natl Acad Sci U S A*. 92:9363-7.

Dull, T., R. Zufferey, M. Kelly, R.J. Mandel, M. Nguyen, D. Trono, and L. Naldini. 1998. A third-generation lentivirus vector with a conditional packaging system. *J Virol*. 72:8463-71.

Goldstein, J.C., F. Rodier, J.C. Garbe, M.R. Stampfer, and J. Campisi. 2005. Caspase-independent cytochrome c release is a sensitive measure of low-level apoptosis in cell culture models. *Aging Cell*. 4:217-22.

Griffith, J.D., L. Comeau, S. Rosenfield, R.M. Stansel, A. Bianchi, H. Moss, and T. de Lange. 1999. Mammalian telomeres end in a large duplex loop [see comments]. *Cell*. 97:503-14.

Gudkov, A.V., C.R. Zelnick, A.R. Kazarov, R. Thimmapaya, D.P. Suttle, W.T. Beck, and I.B. Roninson. 1993. Isolation of genetic suppressor elements, inducing resistance to topoisomerase II-interactive cytotoxic drugs, from human topoisomerase II cDNA. *Proc Natl Acad Sci U S A*. 90:3231-5.

Guiducci, C., M.A. Cerone, and S. Bacchetti. 2001. Expression of mutant telomerase in immortal telomerase-negative human cells results in cell cycle deregulation, nuclear and chromosomal abnormalities and rapid loss of viability. *Oncogene*. 20:714-25.

Hahn, W.C., S.A. Stewart, M.W. Brooks, S.G. York, E. Eaton, A. Kurachi, R.L. Beijersbergen, J.H. Knoll, M. Meyerson, and R.A. Weinberg. 1999. Inhibition of telomerase limits the growth of human cancer cells [see comments]. *Nat Med*. 5:1164-70.

Herbig, U., W.A. Jobling, B.P. Chen, D.J. Chen, and J.M. Sedivy. 2004. Telomere shortening triggers senescence of human cells through a pathway involving ATM, p53, and p21(CIP1), but not p16(INK4a). *Mol Cell*. 14:501-13.

Hockemeyer, D., J.P. Daniels, H. Takai, and T. de Lange. 2006. Recent expansion of the telomeric complex in rodents: Two distinct POT1 proteins protect mouse telomeres. *Cell*. 126:63-77.

Hockemeyer, D., A.J. Sfeir, J.W. Shay, W.E. Wright, and T. de Lange. 2005. POT1 protects telomeres from a transient DNA damage response and determines how human chromosomes end. *Embo J*. 24:2667-78.

Houghtaling, B.R., L. Cuttonaro, W. Chang, and S. Smith. 2004. A dynamic molecular link between the telomere length regulator TRF1 and the chromosome end protector TRF2. *Curr Biol*. 14:1621-31.

Hultdin, M., E. Gronlund, K. Norrback, E. Eriksson-Lindstrom, T. Just, and G. Roos. 1998. Telomere analysis by fluorescence in situ hybridization and flow cytometry. *Nucleic Acids Res*. 26:3651-6.

Iwano, T., M. Tachibana, M. Reth, and Y. Shinkai. 2004. Importance of TRF1 for functional telomere structure. *J Biol Chem*. 279:1442-8.

Karlseder, J., D. Broccoli, Y. Dai, S. Hardy, and T. de Lange. 1999. p53- and ATM-dependent apoptosis induced by telomeres lacking TRF2. *Science*. 283:1321-5.

Kim, S.H., C. Beausejour, A.R. Davalos, P. Kaminker, S.J. Heo, and J. Campisi. 2004. TIN2 mediates functions of TRF2 at human telomeres. *J Biol Chem*. 279:43799-804.

Kim, S.H., S. Han, Y.H. You, D.J. Chen, and J. Campisi. 2003. The human telomere-associated protein TIN2 stimulates interactions between telomeric DNA tracts in vitro. *EMBO Rep*. 4:685-91.

Kim, S.H., P. Kaminker, and J. Campisi. 1999. TIN2, a new regulator of telomere length in human cells [see comments]. *Nat Genet*. 23:405-12.

Li, S., J.E. Rosenberg, A.A. Donjacour, I.L. Botchkina, Y.K. Hom, G.R. Cunha, and E.H. Blackburn. 2004. Rapid inhibition of cancer cell growth induced by lentiviral delivery and expression of mutant-template telomerase RNA and anti-telomerase short-interfering RNA. *Cancer Res*. 64:4833-40.

Liu, D., M.S. O'Connor, J. Qin, and Z. Songyang. 2004a. Telosome, a mammalian telomere-associated complex formed by multiple telomeric proteins. *J Biol Chem*. 279:51338-42.

Liu, D., A. Safari, M.S. O'Connor, D.W. Chan, A. Laegeler, J. Qin, and Z. Songyang. 2004b. PTOP interacts with POT1 and regulates its localization to telomeres. *Nat Cell Biol*. 6:673-80.

Loayza, D., and T. De Lange. 2003. POT1 as a terminal transducer of TRF1 telomere length control. *Nature*. 424:1013-8.

Nair, A.R., M. Schliekelman, M.B. Thomas, J. Wakefield, S. Jurgensen, and R. Ramabhadran. 2005. Inhibition of p53 by lentiviral mediated shRNA abrogates G1 arrest and apoptosis in retinal pigmented epithelial cell line. *Cell Cycle*. 4:697-703.

O'Connor M, S., A. Safari, H. Xin, D. Liu, and Z. Songyang. 2006. A critical role for TPP1 and TIN2 interaction in high-order telomeric complex assembly. *Proc Natl Acad Sci U S A*.

O'Connor, M.S., A. Safari, H. Xin, D. Liu, and Z. Songyang. 2006. A critical role for TPP1 and TIN2 interaction in high-order telomeric complex assembly. *Proc Natl Acad Sci U S A*. 103:11874-9.

Okabe, J., A. Eguchi, R. Wadhwa, R. Rakwal, R. Tsukinoki, T. Hayakawa, and M. Nakanishi. 2004. Limited capacity of the nuclear matrix to bind telomere repeat binding factor TRF1 may restrict the proliferation of mortal human fibroblasts. *Hum Mol Genet*. 13:285-93.

Rodier, F., S.H. Kim, T. Nijjar, P. Yaswen, and J. Campisi. 2005. Cancer and aging: the importance of telomeres in genome maintenance. *Int J Biochem Cell Biol*. 37:977-90.

Smogorzewska, A., and T. De Lange. 2002. Different telomere damage signaling pathways in human and mouse cells. *Embo J*. 21:4338-48.

Smogorzewska, A., and T. de Lange. 2004. Regulation of telomerase by telomeric proteins. *Annu Rev Biochem*. 73:177-208.

Takai, H., A. Smogorzewska, and T. de Lange. 2003. DNA damage foci at dysfunctional telomeres. *Curr Biol*. 13:1549-56.
van Steensel, B., and T. de Lange. 1997. Control of telomere length by the human telomeric protein TRF1 [see comments]. *Nature*. 385:740-3.
van Steensel, B., A. Smogorzewska, and T. de Lange. 1998. TRF2 protects human telomeres from end-to-end fusions. *Cell*. 92:401-13.
Wu, L., A.S. Multani, H. He, W. Cosme-Blanco, Y. Deng, J.M. Deng, O. Bachilo, S. Pathak, H. Tahara, S.M. Bailey, R.R. Behringer, and S. Chang. 2006. Pot1 deficiency initiates DNA damage checkpoint activation and aberrant homologous recombination at telomeres. *Cell*. 126:49-62.
Xin, H., D. Liu, M. Wan, A. Safari, H. Kim, W. Sun, M.S. O'Connor, and Z. Songyang. 2007. TPP1 is a homologue of ciliate TEBP-beta and interacts with POT1 to recruit telomerase. *Nature*. 445:559-62.
Yang, Q., Y.L. Zheng, and C.C. Harris. 2005. POT1 and TRF2 cooperate to maintain telomeric integrity. *Mol Cell Biol*. 25:1070-80.
Ye, J.Z., J.R. Donigian, M. van Overbeek, D. Loayza, Y. Luo, A.N. Krutchinsky, B.T. Chait, and T. de Lange. 2004a. TIN2 binds TRF1 and TRF2 simultaneously and stabilizes the TRF2 complex on telomeres. *J Biol Chem*. 279:47264-71.
Ye, J.Z., D. Hockemeyer, A.N. Krutchinsky, D. Loayza, S.M. Hooper, B.T. Chait, and T. de Lange. 2004b. POT1-interacting protein PIP1: a telomere length regulator that recruits POT1 to the TIN2/TRF1 complex. *Genes Dev*. 18:1649-54.
Zou, Y., A. Sfeir, S.M. Gryaznov, J.W. Shay, and W.E. Wright. 2004. Does a sentinel or a subset of short telomeres determine replicative senescence? *Mol Biol Cell*. 15:3709-18.

Figure Legends

FIGURE 1. Effects of TIN2 ablation on TRF1, TRF2 and cell viability.

a. RNAi reduces TIN2 expression. HT1080 cells were transiently transfected with pSuper vectors expressing shRNAs corresponding to a non-expressed (non-specific, N/S) mRNA or one of three distinct regions in the TIN2 mRNA (T2i-1, T2i-2, T2i-3), as described in Methods. Transfection efficiency varied from 60-70%. Cell lysates were analyzed 48 h later by western blotting for TIN2 expression, with α-tubulin used as a loading control. The protein band intensities were analyzed by the Multi-Gauge program (Fujifilm). TIN2 protein levels were reduced to 23% and 24% of control levels byT2i-2 and T2i-3 respectively. Control cells expressed the non-specific (NS) shRNA.

b. TIN2 reduction decreases TRF1 and TRF2 protein expression. Lysates from HT1080 cells transfected with the N/S (control) or T2i-2 pSuper vectors described above were analyzed for TIN2, TRF1, TRF2 and α-tubulin by western blotting. The protein band intensities were analyzed as described in (a). TIN2 and TRF2 protein levels were reduced to 16% and 13%, respectively, of control levels.

c. TIN2 reduction induces apoptosis in human tumor cells. HT1080 cells were transiently transfected with pSuper vectors containing no insert (Vector) or N/S (control), T2i-1, T2i-2, or T2i-3 shRNAs and analyzed 48 h later for apoptosis as described in Methods. Transfection efficiency was 60-70%. Where indicated, the caspase inhibitor ZVAD (100 μM) was added 8 h after transfection. 200 cells were analyzed for apoptosis in three independent experiments. Error bars represent the standard deviation.

d. TIN2 reduction induces apoptosis in normal human cells. Normal human fibroblasts (HCA2 and WI-38) were transiently co-transfected with pSuper vectors containing no insert (Vector) or T2i-1 or T2i-2 shRNAs, and a lenti-GFP vector at a ratio of 10:1. 48 h later, GFP positive cells were analyzed for apoptosis as described in Methods. Where indicated, WI-38 cells were first infected with a retrovirus expressing GSE-22, selected and then infected with the pSuper and GFP vectors. 200 cells were analyzed in three experiments. Error bars represent the standard deviation.

e. GSE-22 inactivates p53 activity in normal cells.

WI38 cells were infected with a retrovirus expressing GSE-22 or insertless virus, selected, plated and then irradiated with 10 Gy X-ray. The cells were fixed 19 hrs later and immunostained for p21 and p53. Bars, ~ 10 μM.

FIGURE 2. TIN2-mediated complexes.

a. Endogenous TIN2-complexes in HeLa nuclear lysate. Telomeric proteins in HeLa nuclear extracts (2. 5 ml) were fractionated on a Sepharcryl S-300 HR column and immunobloted for the indicated proteins. 20 μl aliquots of the indicated fractions were loaded. Eluting fractions were collected from the

column after the void volume (No. 13). Molecular sizes indicated were derived from a standard curve based on the elution standards, as described in Methods.

b. Western blotting signals in Fig. 2C were quantified with the Multi-Gauge program (Fuji film). Relative band intensities for each protein were plotted.

c. TIN2-complexes. We prepared lysates from HT1080 cells that transiently expressed V5-tagged POT1 and stably expressed FLAG-TIN2 (lanes 2, 4, 6, 8) or HA-TRF1 (1, 10) or both Flag-TIN2 and HA-TRF1 (Kim et al., 1999) (lanes 3, 5, 7, 9, 11). We isolated TIN2 complexes using FLAG, V5 and HA antibodies and analyzed the lysates (10%, Input) and immunoprecipitates (IP) for the indicated proteins by western blotting (WB).

d. Proposed TIN2 complexes. Complex A, TIN2-TRF1; complex B, TIN2-TRF2/hRap1-TPP1/POT1; complex C, TRF1-TIN2-TRF2/hRap1-TPP1/POT1.

FIGURE 3. TIN2 complexes disrupted by TIN2 mutants

a. TIN2 deletion mutants. Wild type TIN2 (aa 1-354) showing N-terminal (N-term), TRF1-interaction (TRF1-Int) and C-terminal (C-term) domains, and deletion mutants TIN2-13 (aa 180-354) and TIN2-15C (aa 1-257).

b. Interaction of TIN2-15C with POT1/TPP1. Lysates from HT1080 cells that transiently expressed Myc-TIN2-15C, V5-POT1 and HA-TRF1 were precipitated using anti-Myc or V5 antibodies. Unprecipitated lysates (10%) and the immune precipitates (IP) were analyzed for POT1-V5, TIN2-15C, TRF2 and HA-TRF1 by western blotting (WB).

c. TIN2-TRF2-POT1 complexes disrupted by TIN2-15C, but not TIN2-13. Lysates from HT1080 cells transiently expressing wild-type (WT)-TIN2, control vector, TIN2-13 or TIN2-15C and V5-POT1 were immunoprecipitated (IP) by anti-V5. The lysates (15%, Input) and immune precipitates were analyzed for TIN2, V5, TRF2 and α-tubulin by western blotting (WB) (lanes 1-8). The band indicated by * is a degraded WT-TIN2 product.

d. TRF1-TIN2 complexes disrupted by TIN2-13, but not TIN2-15C. Lysates from HT1080 cells transiently expressing WT-TIN2, TIN2-13 and TIN2-15C

and HA-TRF1 were immunoprecipitated (IP) by anti-HA. The lysates (15%, Input) and precipitates were analyzed for TIN2, TRF2, HA and α-tubulin by western blotting (WB) (lanes 9-18). The precipitating heavy chain is indicated (IgG). The band indicated by * is a degraded WT-TIN2 product.

FIGURE. 4. Effects ofTIN2 mutants in presenescent and senescent cells.

a. Cell death caused by TIN2-15C in presenescent cells. Where indicated, presenescent (P) HCA2 cells were first infected with a retrovirus expressing GSE-22 and a lenti-virus expressing sh-p53 and selected for 2-3 d. Cells were then infected with lentiviruses expressing GFP, TIN2-13 or TIN2-15C. Where indicated, senescent (S) HCA2 cells were first infected with lentiviruses expressing GFP, TIN2-13 or TIN2-15C, and then infected with lentivirus expressing GSE-22. Cells were scored for apoptotic death by assessing release of cytochrome c from mitochondria as described (Goldstein et al., 2005). 300 cells were scored in 2 or 3 independent experiments. Error bars represent the standard deviation.

d. b. Effects of TIN2-15C on senescent cells reactivated by GSE-22. 5 x 10^4 senescent HCA2 cells were infected with lentiviruses expressing GFP (control), TIN2-13, TIN2-15C or DN-TRF2, and then infected with lenti-GSE-22. Colonies were stained at the indicated days after infection.

c. Expression levels of TIN2 mutants and DN-TRF2. Lysates from presenescent cells infected with the indicated lentiviruses were analyzed for TIN2 and TRF2 by western blotting (WB).

Cell death induced by TIN2-15C in p53-positive and p53-negative cancer cells. p53-positive (breast MCF-7, prostate LN-Cap) cancer cells, and p53-negative (breast MDA-MB-231 and MDA-MB-157, prostate PPC-1 , fibrosarcoma HT1080) cancer cells were transiently transfected with pIRES2-eGFP vectors expressing no insert (vector), TIN2-13 or TIN2-15C. 48 h later, the cells were analyzed for GFP fluorescence. GFP-positive cells were scored for cell death by collapse of the mitochondrial membrane potential as described (Davalos and Campisi, 2003). 200 GFP positive cells were scored

in 2 or 3 independent experiments for each transfection. Error bars represent the standard deviation.

FIGURE. 5. Effects of TIN2 mutants in normal cells.

a. TIN2-15C suppresses proliferation of normal cells. We infected presenescent HCA2 cells with lentiviruses expressing GFP, wild-type (wt) TIN2, TIN2-13 or TIN2-15C and determined cell number the indicated number of days thereafter. Plotted are cumulative cell numbers vs days in culture.

b. TIN2-15C induces cellular senescence. HCA2 cells were infected with lenti-GFP or lenti-TIN2-15C and assessed 10 d later for senescence-associated β-galactosidase, as described (Dimri et al., 1995). Replicatively senescent HCA2 cells were used as positive controls.

e. c. TIN2-13 and TIN2-15C induces damage foci in presenescent and senescent cells. Presenescent (P) and senescent (S) HCA2 cells were infected with lenti-TIN2-13 or lenti-TIN2-15C and stained 48 h later for expression of the mutant proteins and γH2AX or 53BP1 foci. 50-80 cells were scored in 2 or 3 independent experiments for each transfection. Error bars represent the standard deviation.

FIGURE 6.

a. Telomerase does not rescue cell death by TIN2-15C. 5×10^4 senescent cells were infected with lentiviruses expressing GFP (control), the telomerase catalytic subunit hTERT, TIN2-15C or both TIN2-15C and hTERT. The cells were then infected with lenti-GSE-22. After 2 d, the cells were subcultured and plated for colony formation. Colonies were fixed and stained 61 days later.

b. Colonies were counted 5, 11 and 61 days after plating. Colonies were scored in 2 or 3 independent experiments for each transfection. Error bars represent the standard deviation.

c. Proposed model for TIN2 complexes at telomeres.

Complex A and B cooperate, albeit at different positions on telomeres, to form t-loops or other terminal structures. Complex B may localize preferentially or uniquely near t-loop junctions, whereas A complexes may modulate the tertiary structure of telomeres and promote B complex stability. TIN2-13 disrupts complex A, thereby reducing the tertiary telomeric structure and destabilizing B complexes, resulting in partial or mild disruption of t-loops and telomere uncapping. TIN2-15C directly disrupts B complexes, resulting in severe disruption of t-loops and telomere uncapping. Cells expressing wild type p53 and TIN2-13 or TIN2-15 undergo growth arrest, whereas cells lacking functional p53 undergo cell death. In both cases, the consequences of TIN2-15C expression are more severe than that of expressing TIN-13.

Table 1.

Presenescent HCA2 cells were infected with a retroviruses expressing GSE-22, selected and then infected with lentiviruses expressing GFP, TIN2-13 or TIN2-15C. The cells were treated with colcemid and telomeres on metaphase chromosomes were identified by PNA-FISH, as described in Experimental procedures. Chromosome fusions were scored by fluorescence in situ hybridization for the presence (+Tel.) or absence (-Tel) if telomeric DNA at the site of fusion.

TABLE 1. Telomeric fusions caused by expression of TIN2 mutants.

Lentiviral vector	No. Metaphases analyzed	No. Chromosome fusions +Tel	–Tel	Fusions/ metaphase	Fusions/ chromosome
GFP	53	0	0	0	0
TIN2-13	53	7	3	0.18	0.0034
TIN2-15C	61	42	10	0.85	0.0175

Supplementary Figure 1. TIN2 reduction decreases TRF1 and TRF2 foci.

HT1080 cells transfected with the N/S (control) or T2i-2 pSuper vectors were immunostained for TIN2 and TRF1 (left panels) or TRF2 (right panels). Arrowheads indicate nuclei (visible by DAPI) that lack TIN2 and TRF1 (left panels) or TRF2 (right panels) immunostaining. Transfection efficiency was 60-70%. Bars, ~ 10 μM.

a. **Supplementary Figure 2. Additional fractionation of TIN2-TRF1 complexes from HeLa cell nuclear lysate and efficiency of our nuclear extraction protocol.**

HeLa cell nuclear extracts (5 ml) were fractionated on a Superdex S-200 HR (Pharmacia) column as described in Experimental Procedures and analyzed for the indicated proteins by western blotting. 20 μl aliquots of the indicated fractions were loaded. Each fraction after the column void volume (fraction 13) was collected and analyzed. Molecular sizes were derived from a standard curve based on the elution of standards described in Material and Methods.

Nuclear extraction efficiently liberates telomeric proteins. To assess the efficiency of our extraction protocol, exponentially growing HeLa cells (1L) were serially extracted, maintaining equivalent buffer/cell ratios for all steps. Nuclear extraction yielded a cytoplasmic fraction (lane 1), nuclear extract (lane2) and insoluble pellet. The insoluble pellet was further extracted by sonication and DNAse I treatment (2h, 25 °C) in nuclear extraction buffer supplemented with 5mM CaCl and MgCl (lane 3). The remaining pellet was resuspended in SDS buffer, sonicated, and boiled for 10 min. Equivalent volumes of each fraction were analyzed by western blotting for the indicated proteins.

Supplementary Figure 3. Telomeric G-strand overhangs and telomere length analyses.

a. We transfected HCA2 cells with a tetracycline-inducible lentiviral vector containing no insert (vector) or a TIN2-15C cDNA and treated these cells or not with tetracycline (1 μg/ml) for 3 d. We also infected HCA2 cells with a retroviral vector expressing no insert (vector) or DN-TRF2 for 3d. We isolated and analyzed DNA, with or without treatment of Exonuclease I , by hybridizing with a C-strand telomeric probe after separation in non-denaturing gels to detect the telomeric 3'-overhangs (left panels) or in denaturing gels to detect total telomeric DNA (right panels). DNA signals were quantified with the Multi-Gauge program (FLA-7000, Fuji film). Signals from the denaturing gel were used to normalize the signals from the non-denaturing gel, and the results were expressed in arbitrary units.

b. Induction of TIN2-15C or expression of DN-TRF2 was confirmed by western analysis.

Supplementary Figure 4. Telomeric damage response. HCA2 cells infected with lentiviruses expressing TIN2-15C or TIN2-13 were co-stained for telomeric DNA, using fluorescence *in situ* hybridization and a protein nucleic acid probe, and 53BP1 foci.

Supplementary Figure 5. **Telomeric fusions and anaphase-bridges in cells expressing TIN2-15C.**

a. Telomeres were visualized by fluorescence *in situ* hybridization (FISH) on metaphase spreads using a telomeric protein nucleic acid (PNA) probe. Telomere fusions as indicated by the yellow arrow were detected by superimposing the telomere image on the DAPI-stained chromosome image. Examples are shown of chromosome fusions with (1, 2 and 3) or without (4) telomeric DNA at the sites of fusion, and a circular fusion (3).

As shown for the cell death analyses in Figure 4a, presenescent HCA2 cells were first infected with a retrovirus expressing GSE-22 or a lenti-virus expressing sh-p53 and then infected with lentiviruses expressing GFP, TIN2-13 or TIN2-15C. Cells were treated with the caspase inhibitor (QVD) as

described (Goldstein et al., 2005). Anaphase bridges and micronuclei were quantified after DAPI staining. ~200 cells were scored in 2 or 3 independent experiments for each transfection. Error bars represent the standard deviation.

Figure 1 abcde

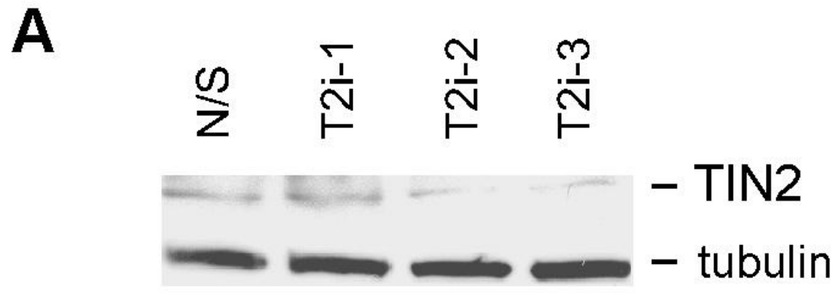

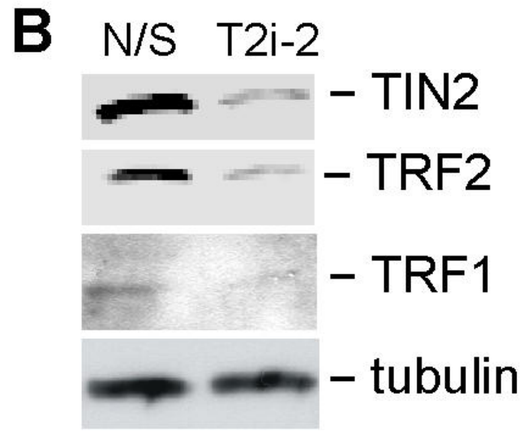

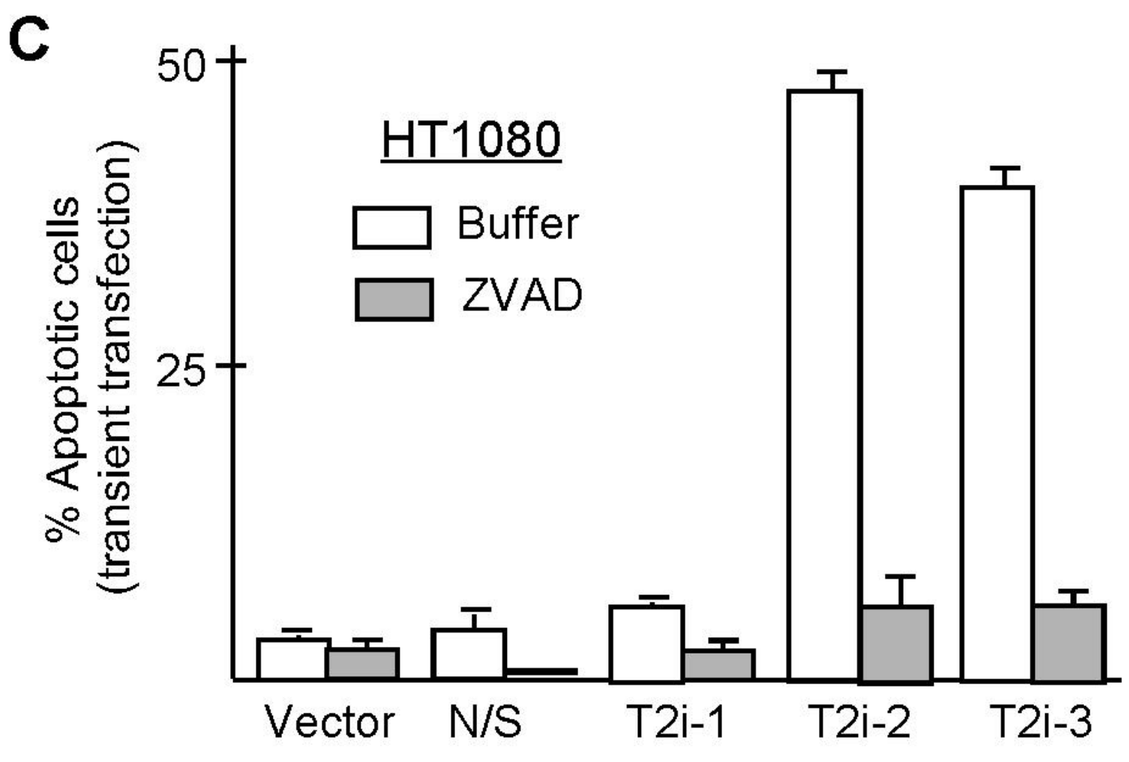

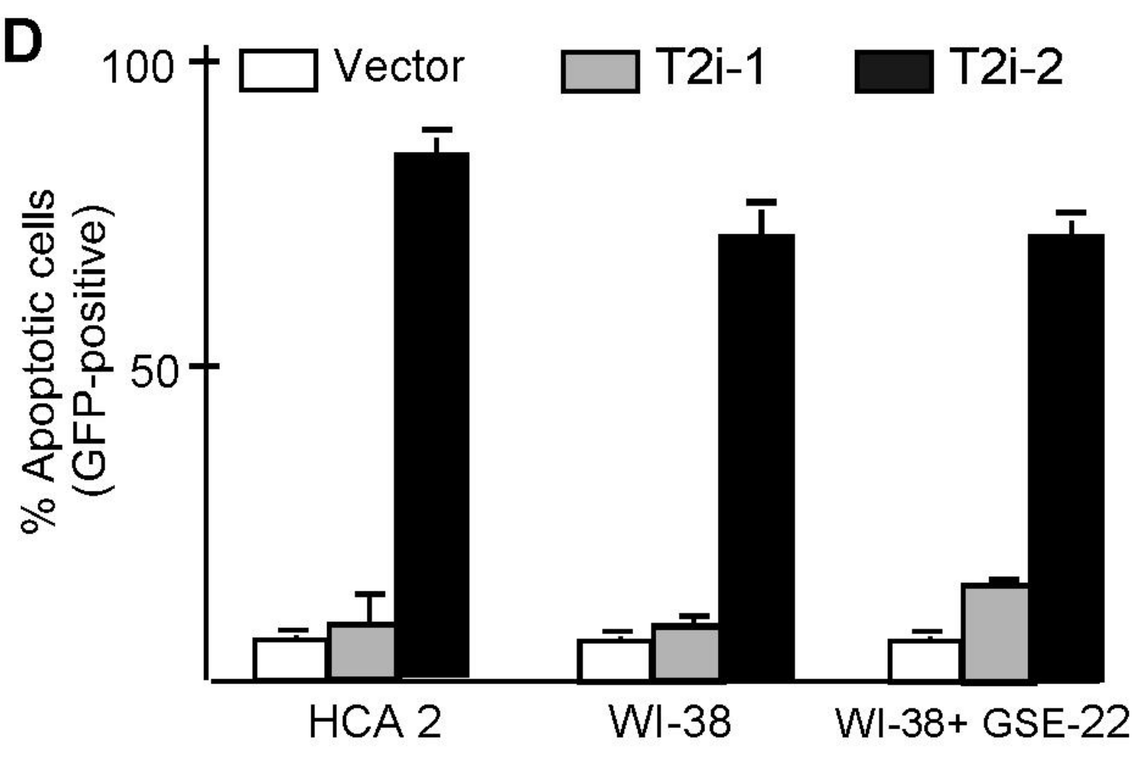

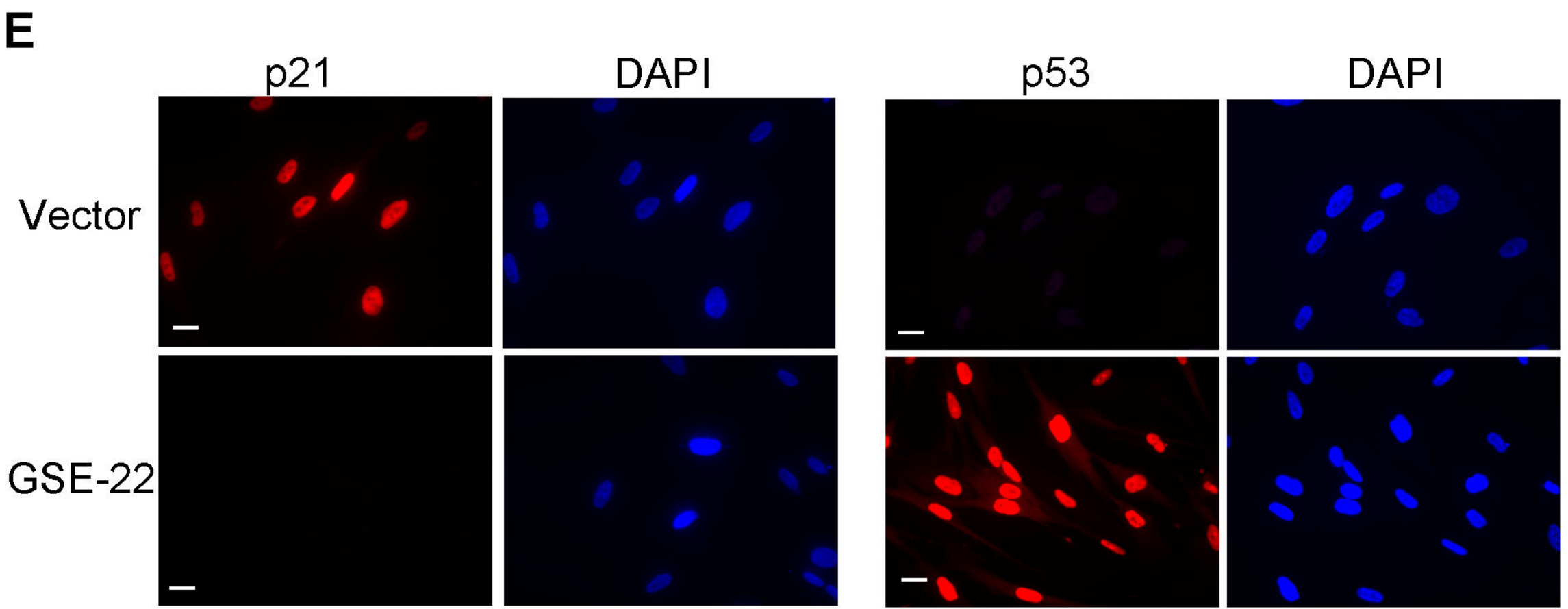

a

Fig2AB

A

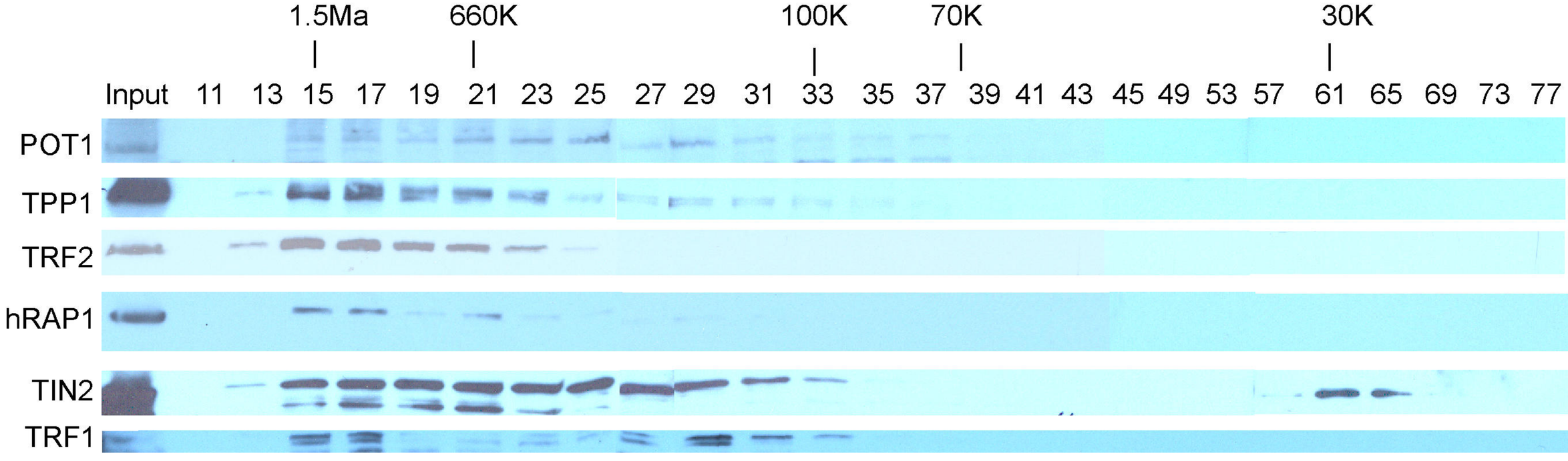
1.5Ma
660K
100K
70K
30K
Input 11 13 15 17 19 21 23 25 27 29 31 33 35 37 39 41 43 45 49 53 57 61 65 69 73 77
POT1
TPP1
TRF2
hRAP1
TIN2
TRF1
Complex C/ shelterin
Complex B
Complex A
POT1/TPP1

B

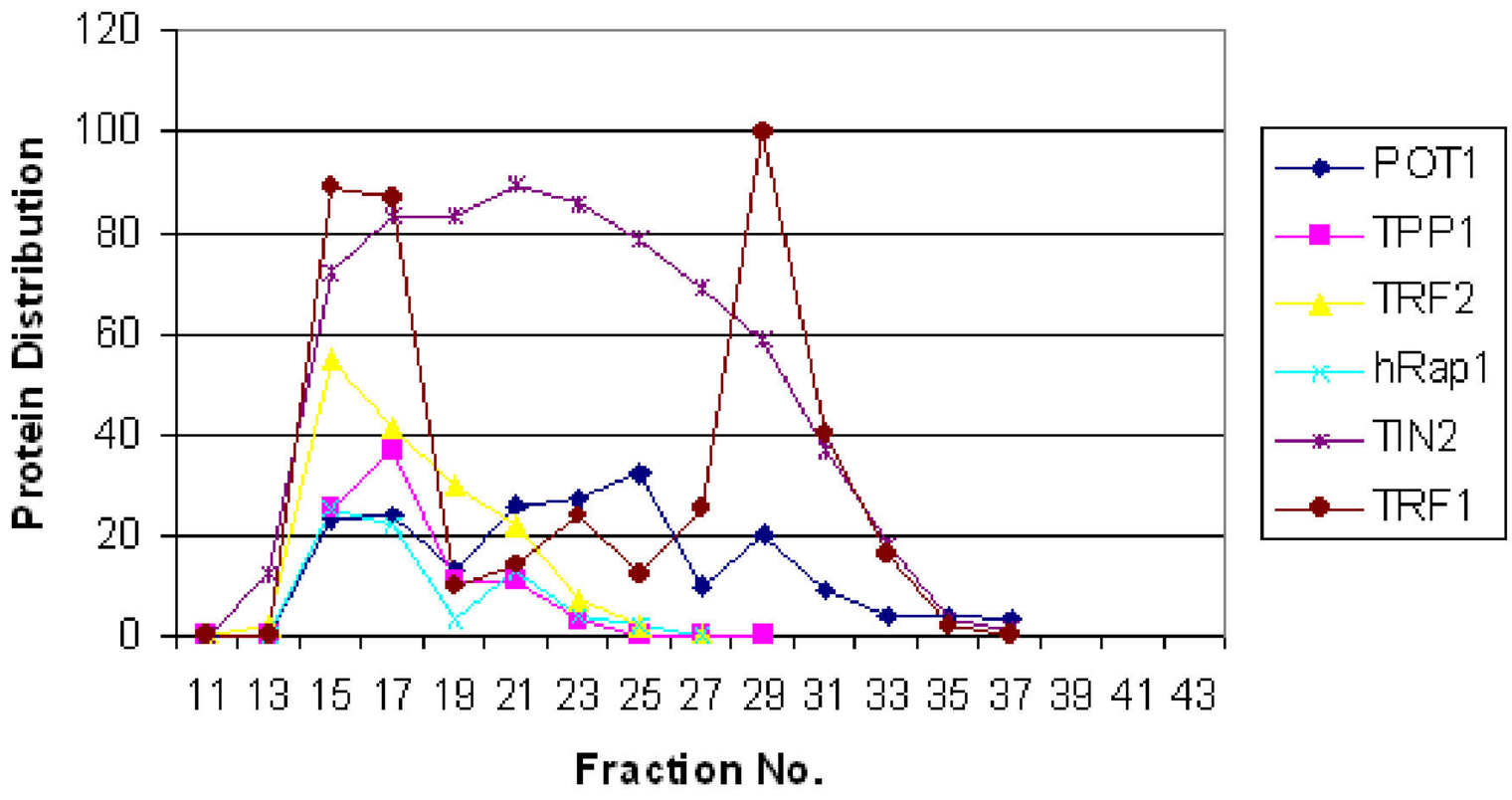
Protein Distribution
120
100
80
60
40
20
0
11 13 15 17 19 21 23 25 27 29 31 33 35 37 39 41 43
Fraction No.
POT1
TPP1
TRF2
hRap1
TIN2
TRF1

Fig. 2CD

C

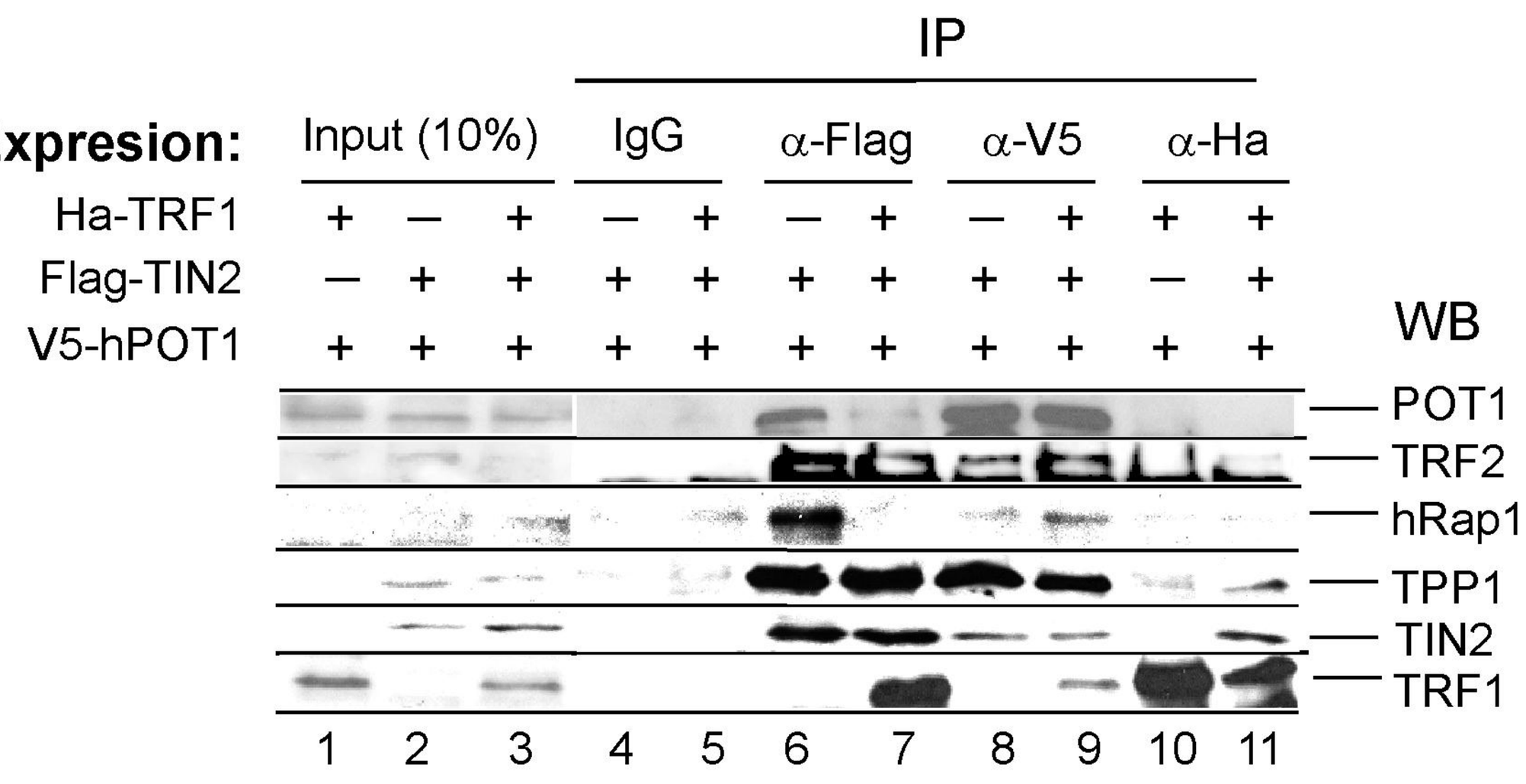
IP
Expresion:
Input (10%)
IgG
α-Flag
α-V5
α-Ha
Ha-TRF1 + — + — + — + — + — + +
Flag-TIN2 — + + + + + + + + — +
V5-hPOT1 + + + + + + + + + + +
WB
POT1
TRF2
hRap1
TPP1
TIN2
TRF1
1 2 3 4 5 6 7 8 9 10 11

D

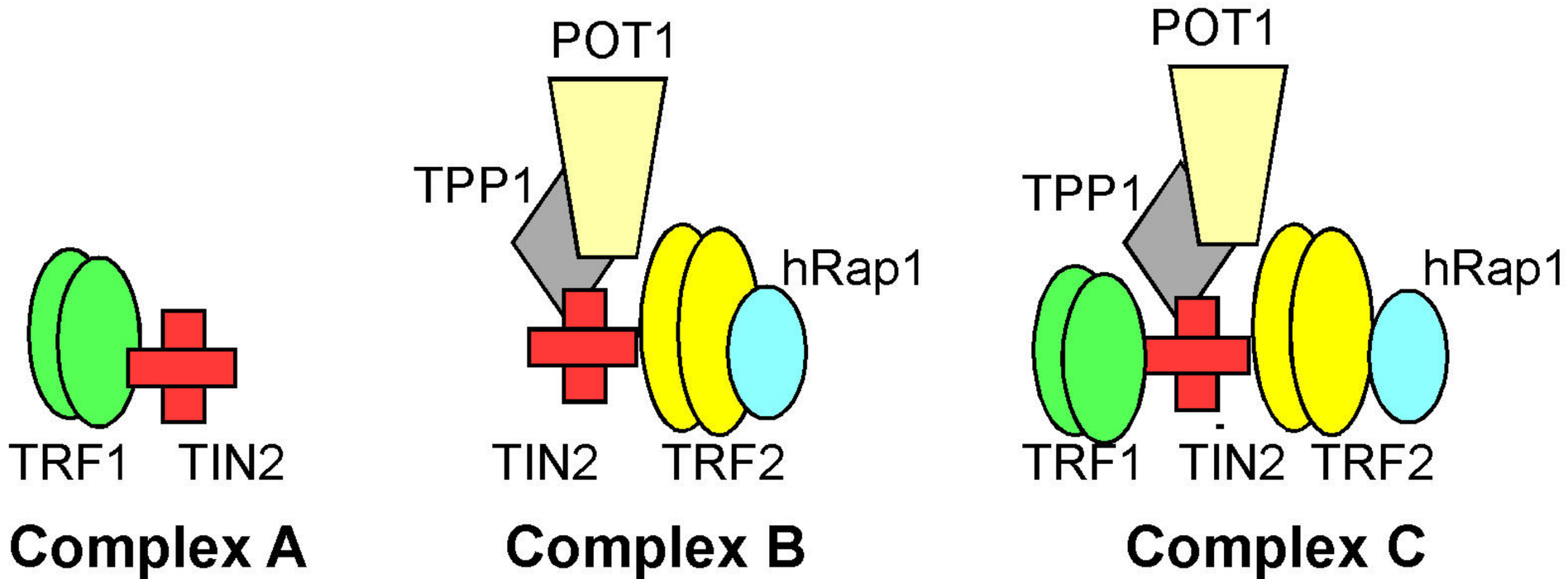
TRF1
TIN2
Complex A
POT1
TPP1
hRap1
TIN2
TRF2
Complex B
POT1
TPP1
hRap1
TRF1
TIN2
TRF2
Complex C

Fig 3ABCD

A

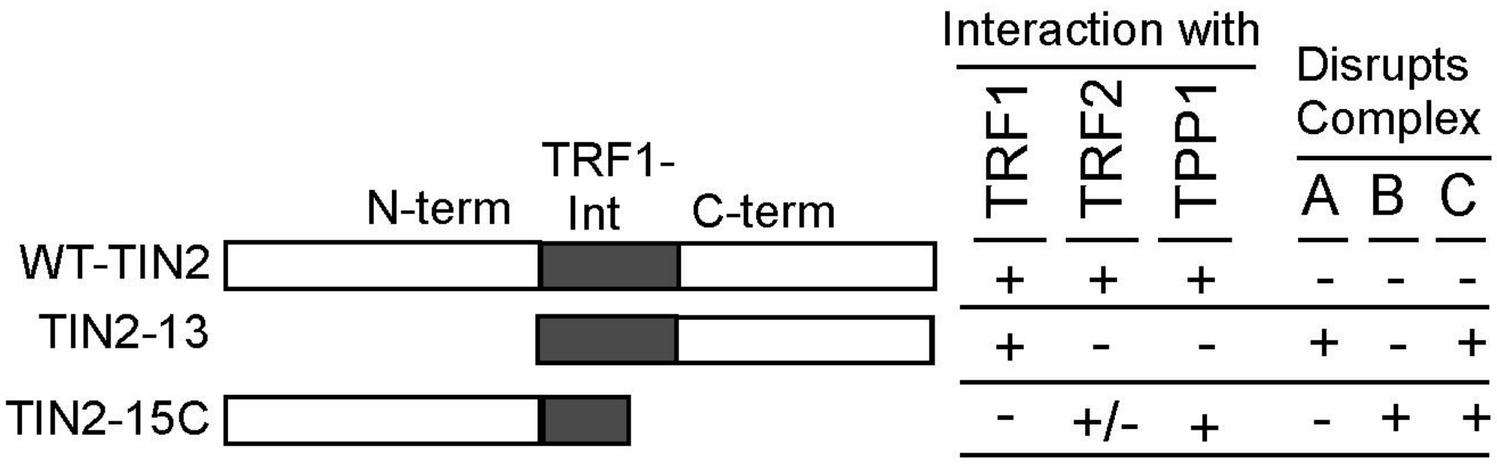

B

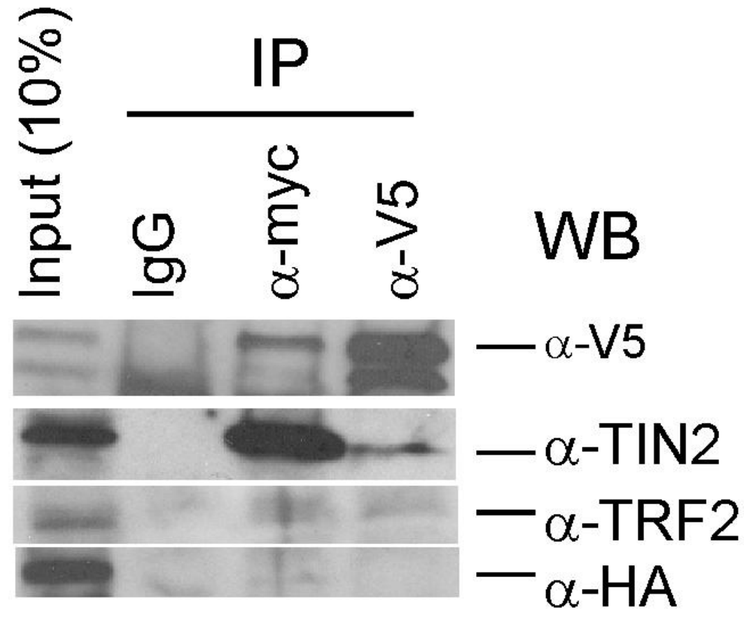

C

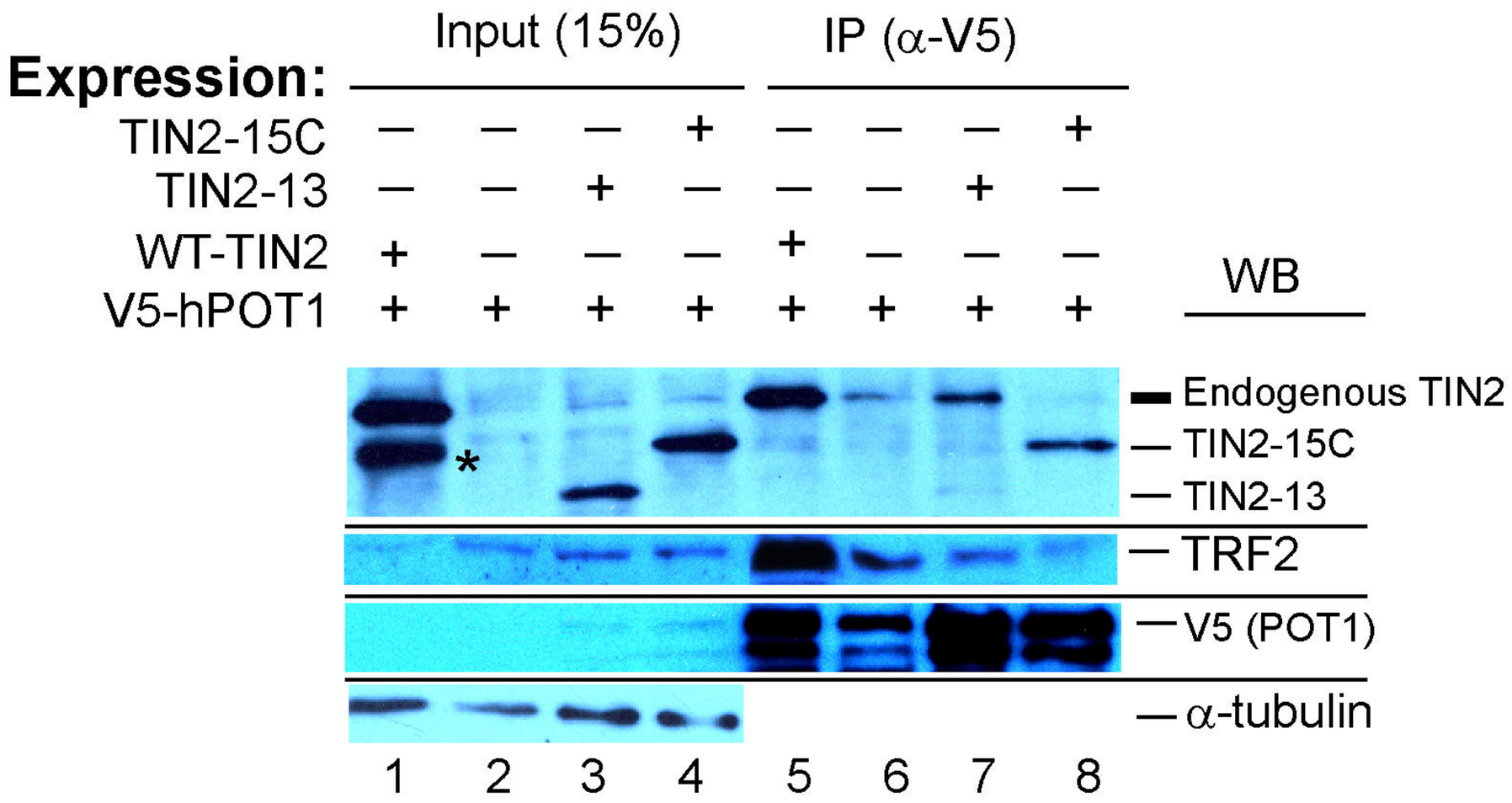

D

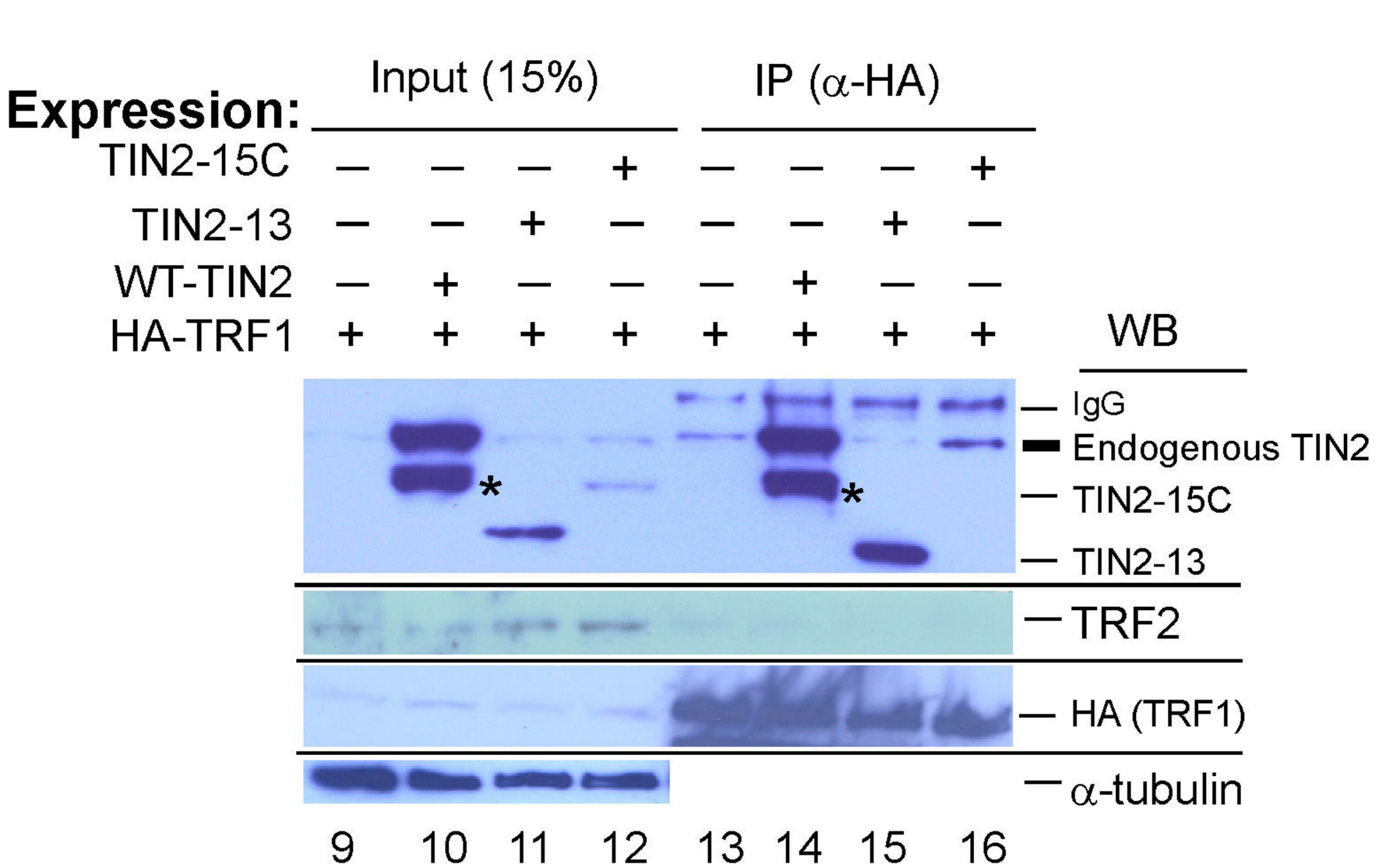

Fig 4.ABCD

A

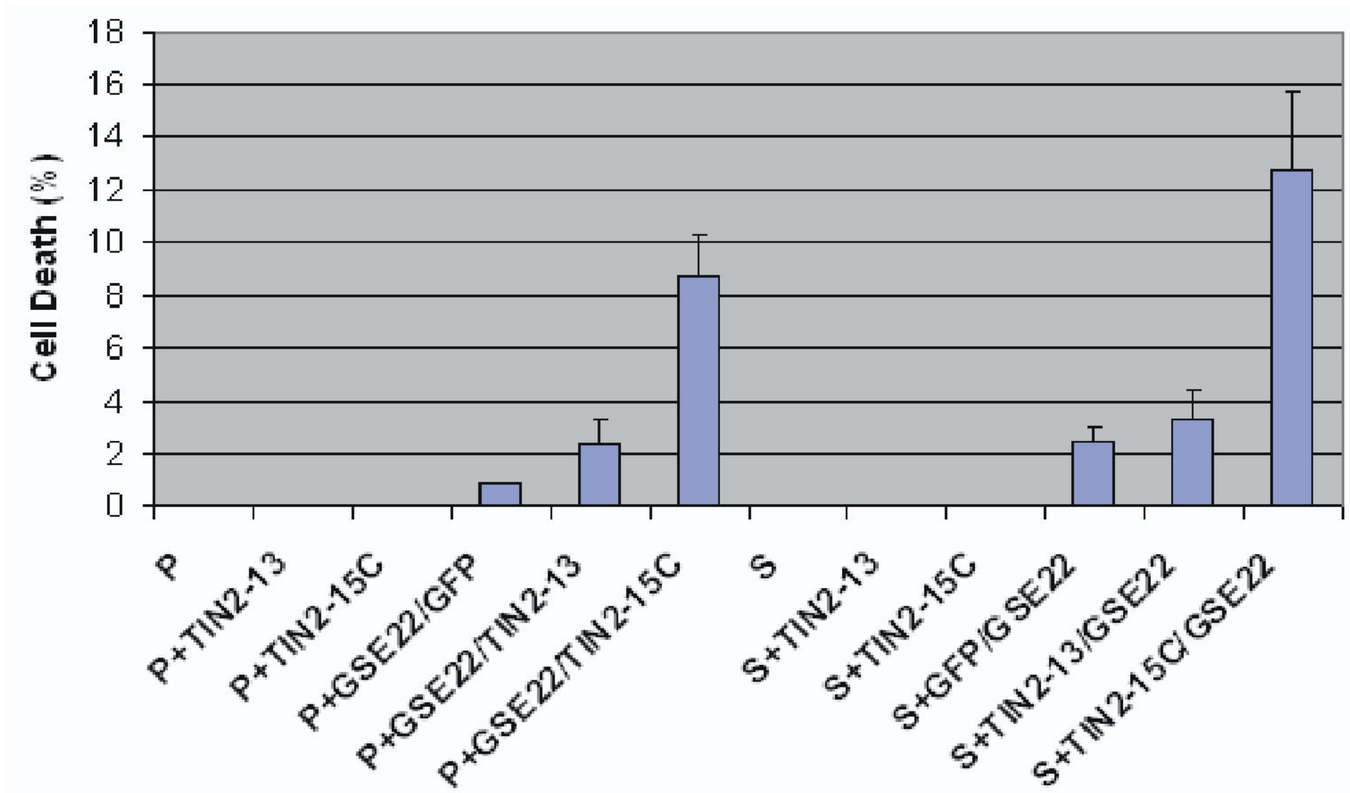

B

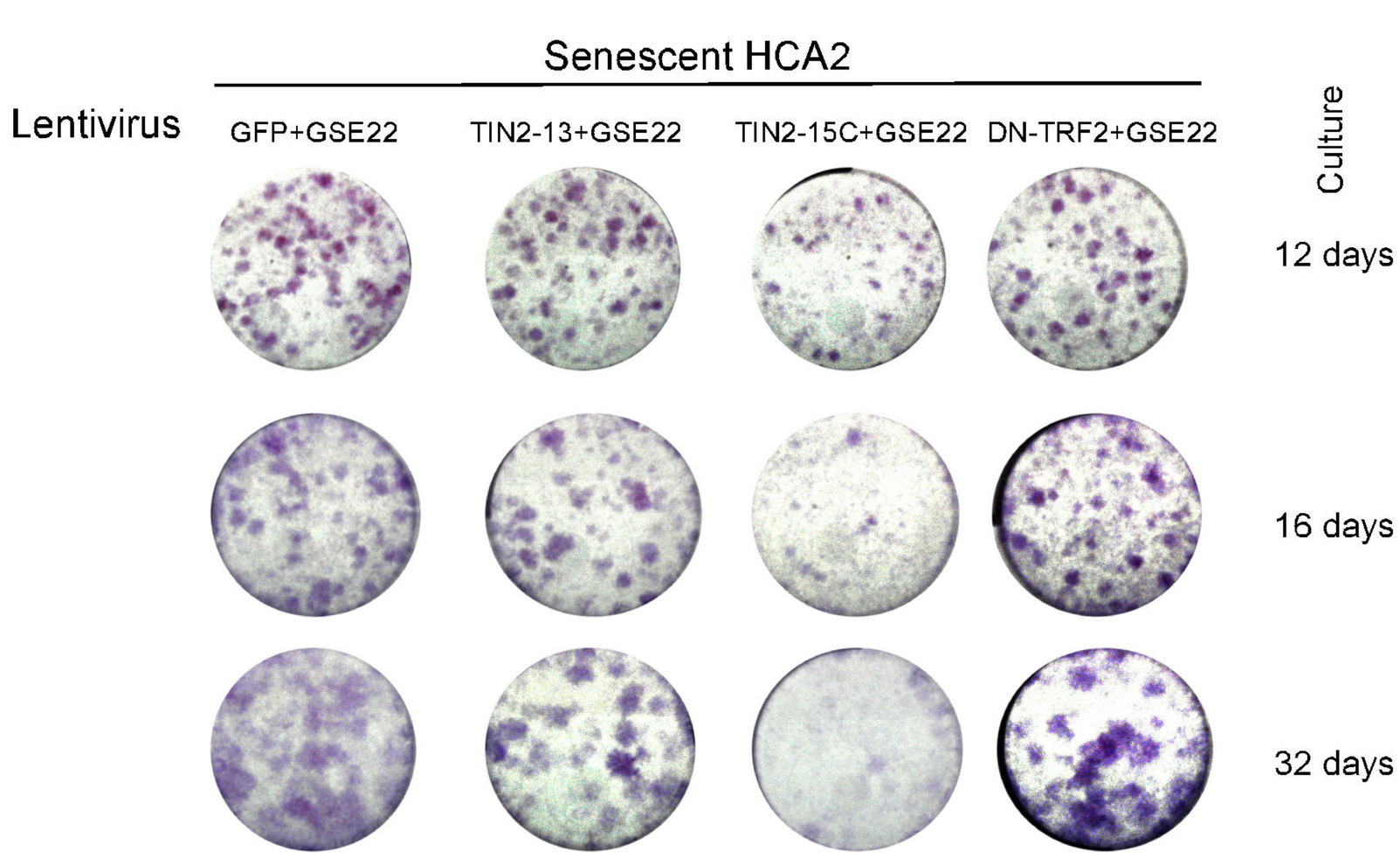

C

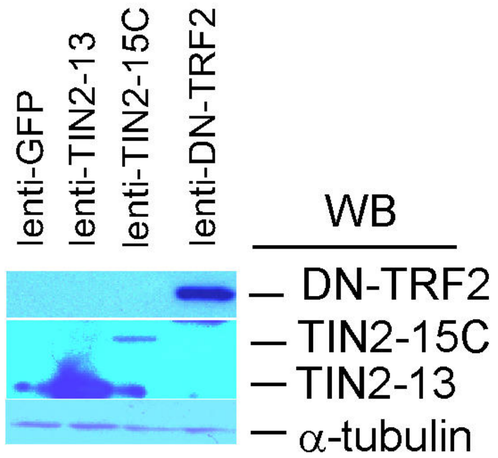

D

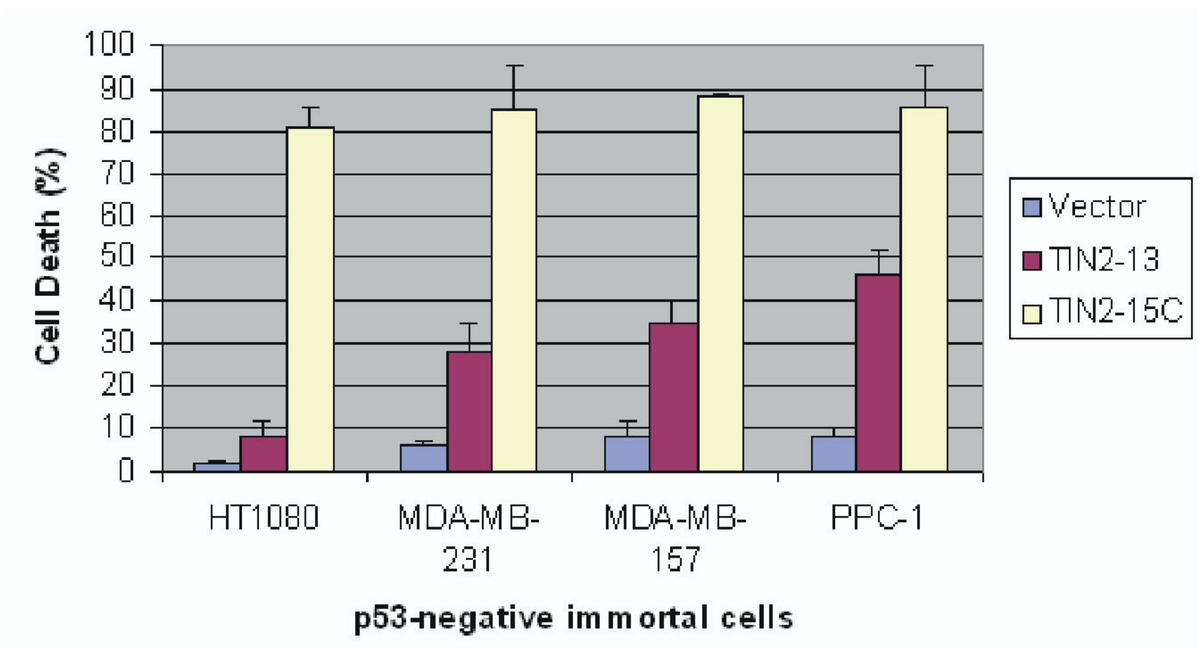

Fig.5ABC

A

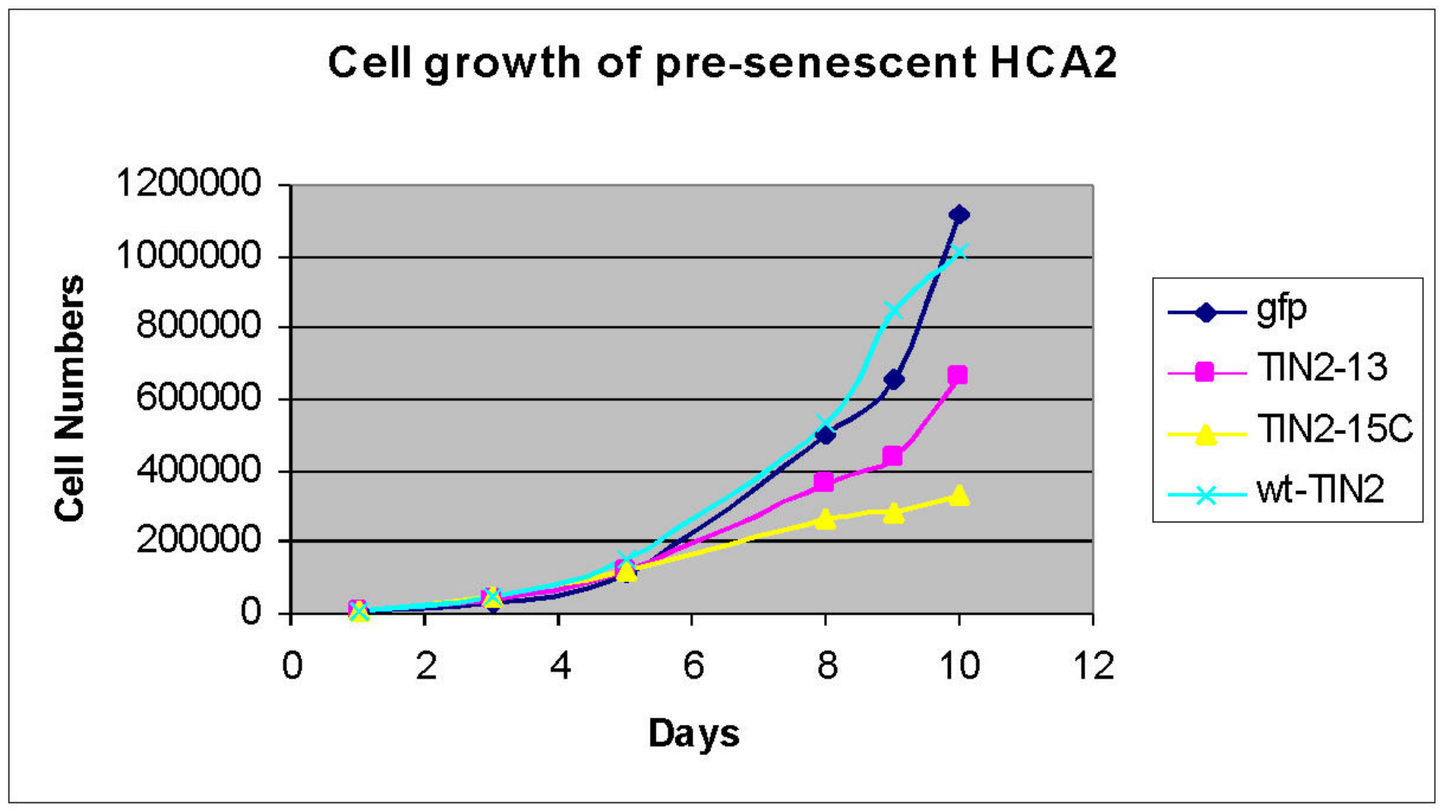
Cell growth of pre-senescent HCA2
Cell Numbers
1200000
1000000
800000
600000
400000
200000
0
0
2
4
6
8
10
12
Days
gfp
TIN2-13
TIN2-15C
wt-TIN2

B

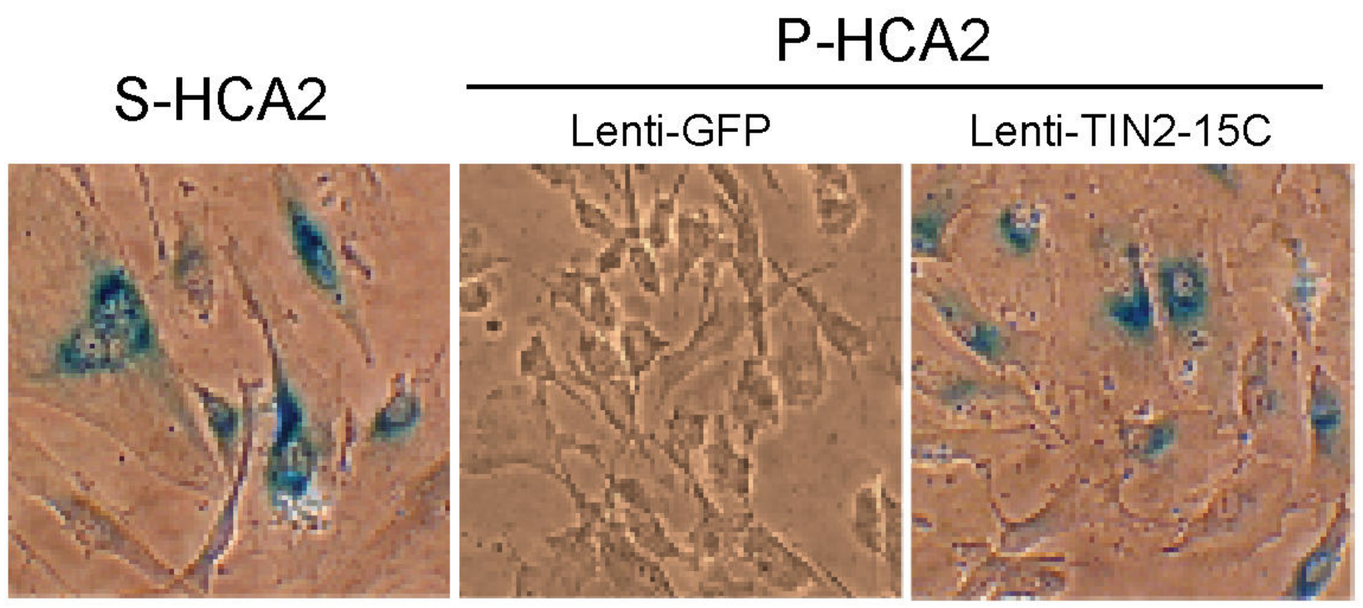
S-HCA2
P-HCA2
Lenti-GFP
Lenti-TIN2-15C

C

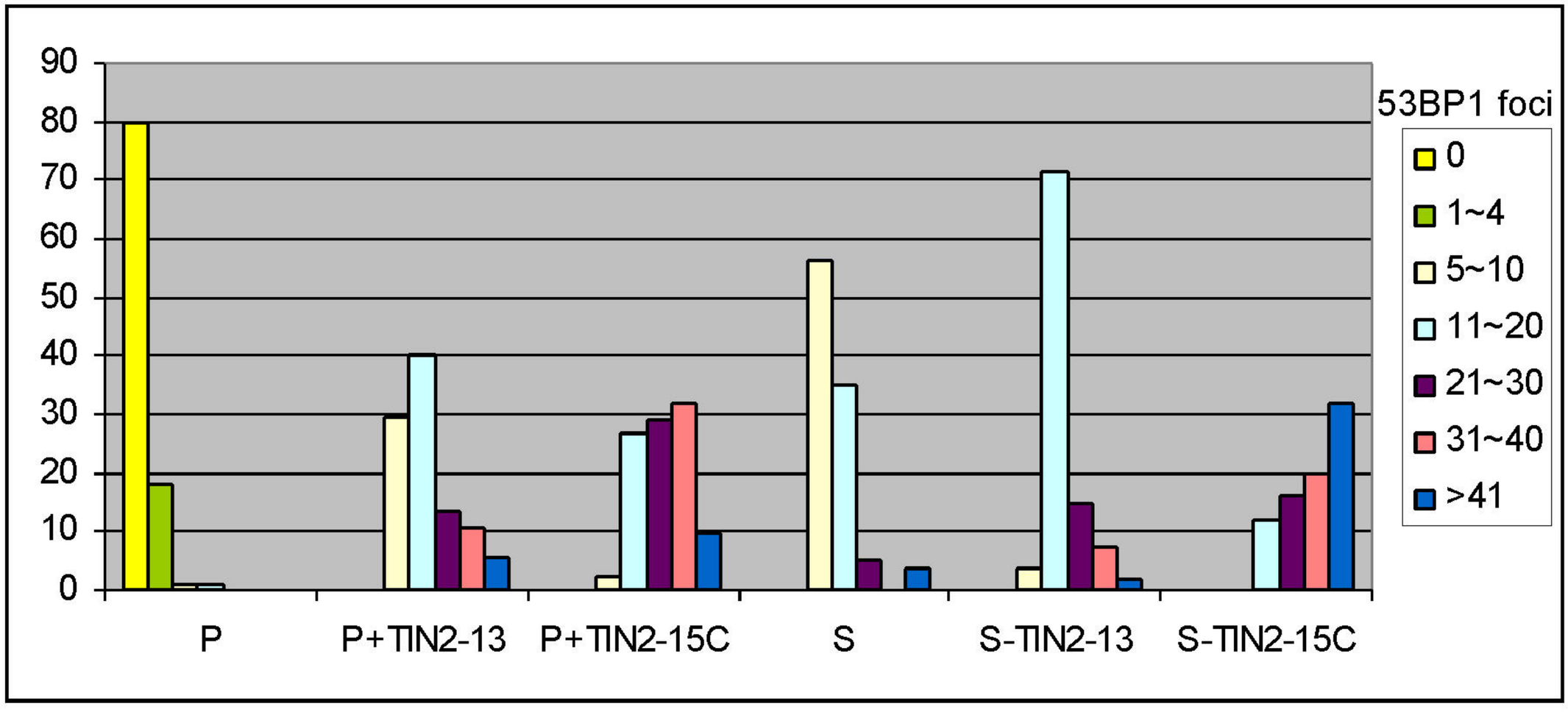
90
80
70
60
50
40
30
20
10
0
P
P+TIN2-13
P+TIN2-15C
S
S-TIN2-13
S-TIN2-15C
53BP1 foci
0
1~4
5~10
11~20
21~30
31~40
>41

Fig 6ABC

A

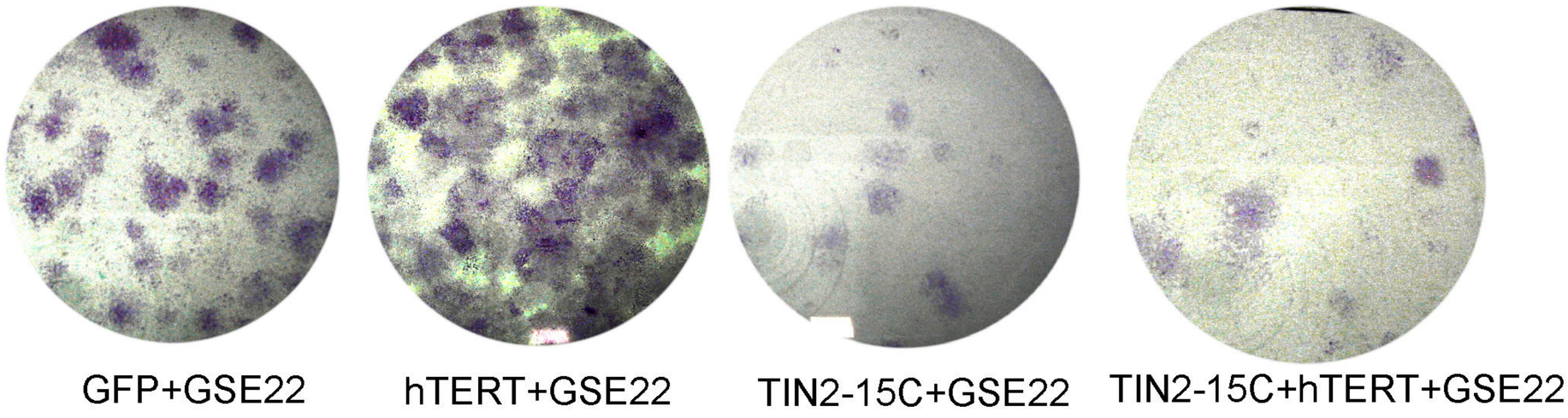

GFP+GSE22 hTERT+GSE22 TIN2-15C+GSE22 TIN2-15C+hTERT+GSE22

B

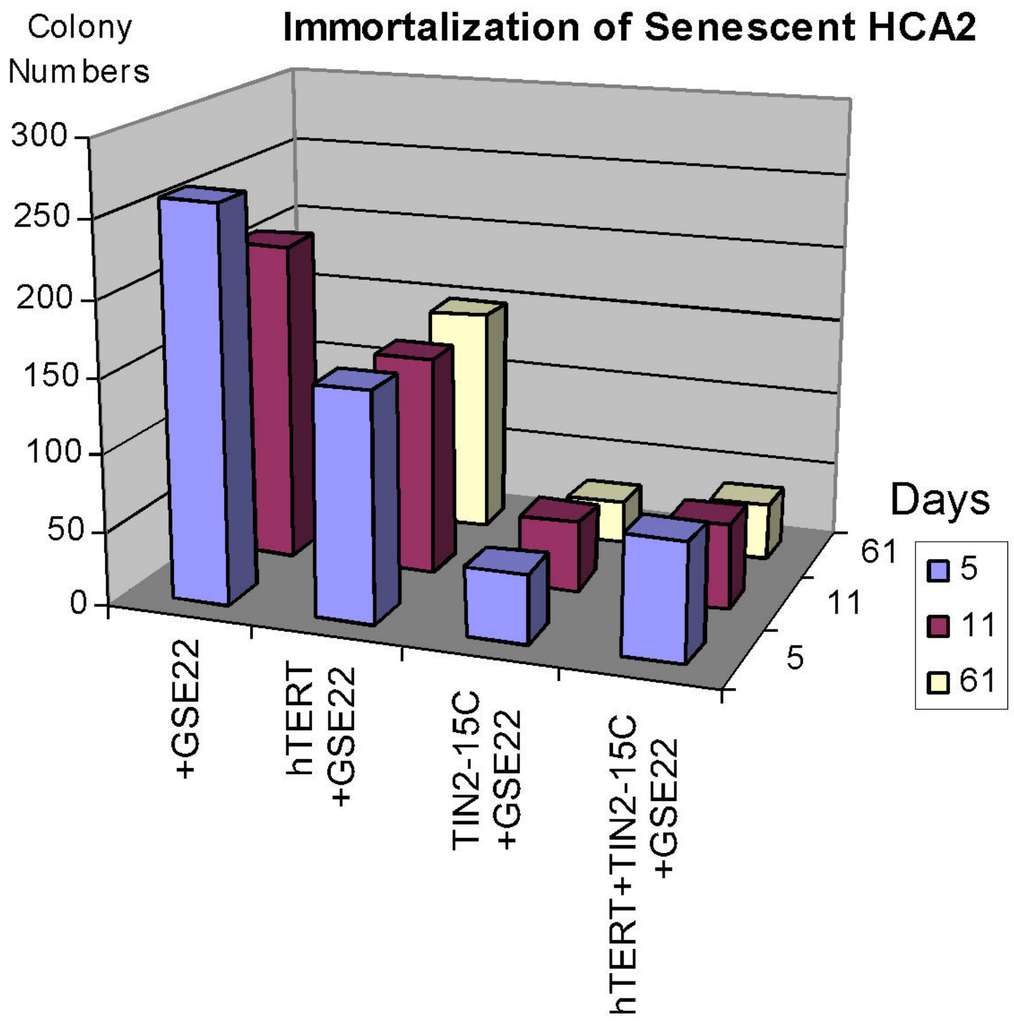

C

Suppl. Figure 1

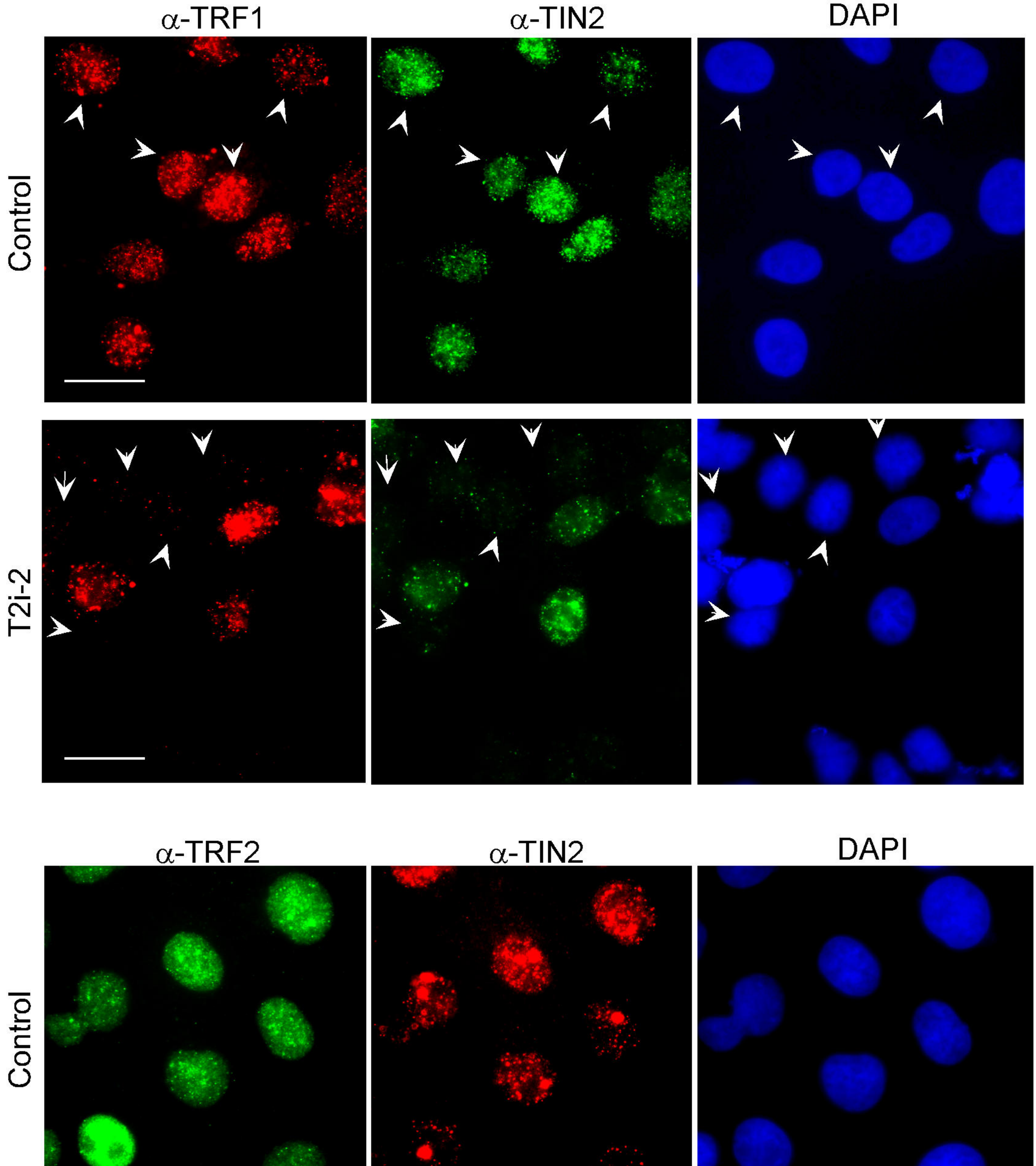

Supplementary Figure 2

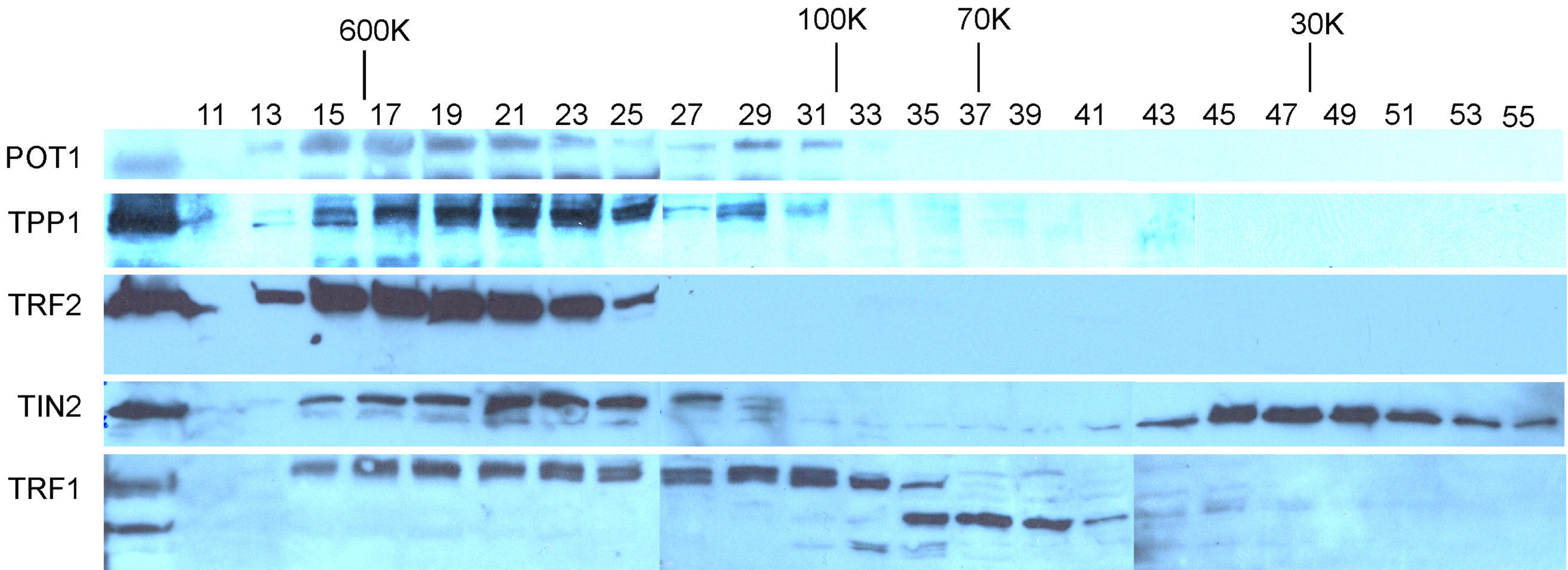

Suppl. Fig. 3

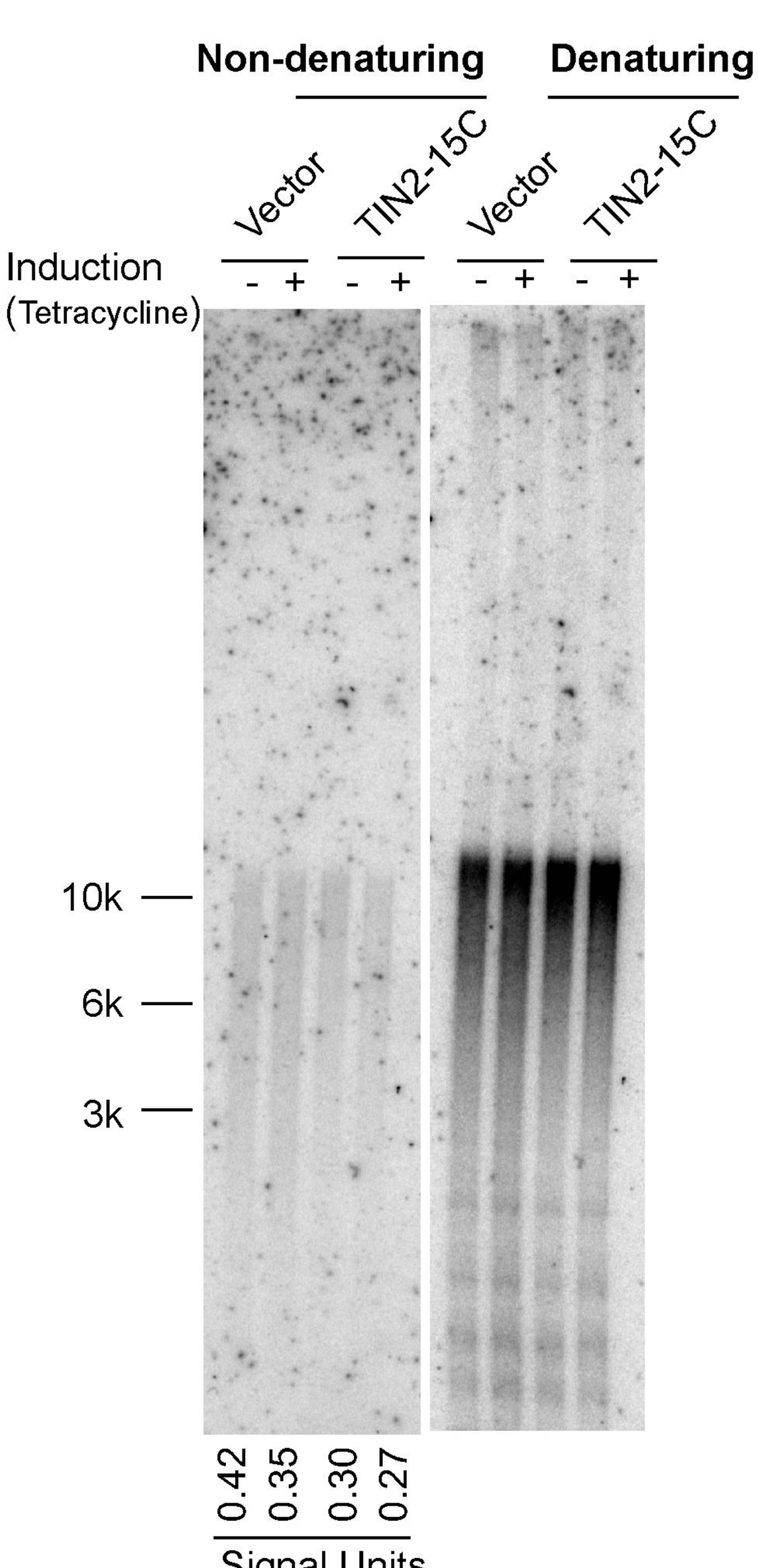
A
Non-denaturing
Denaturing
Vector
TIN2-15C
Vector
TIN2-15C
Induction
(Tetracycline)
- + - + - + - +
10k
6k
3k
0.42
0.35
0.30
0.27
Signal Units

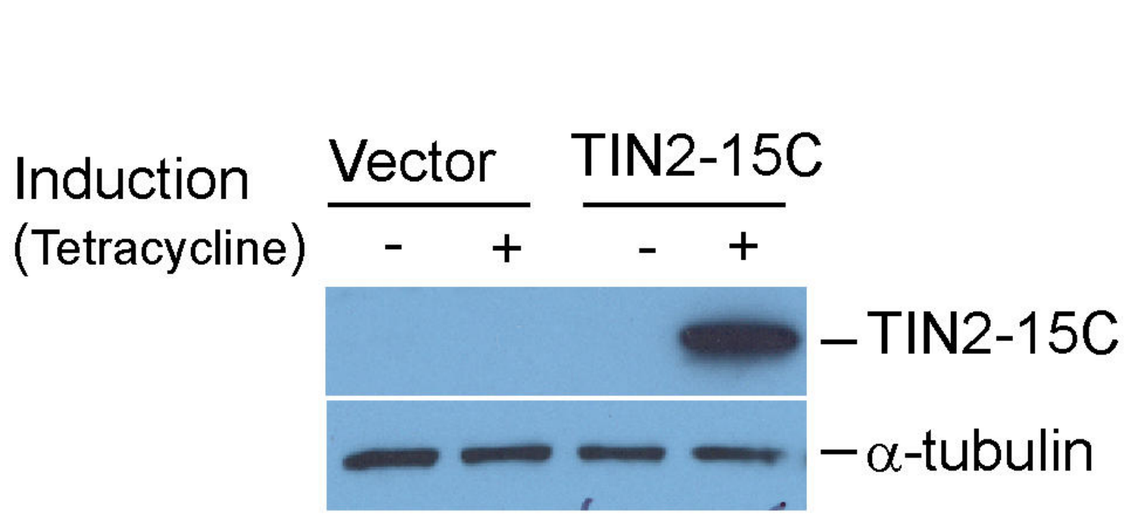
B
Induction
(Tetracycline)
Vector
TIN2-15C
- + - +
TIN2-15C
α-tubulin

Suppl. Fig. 4

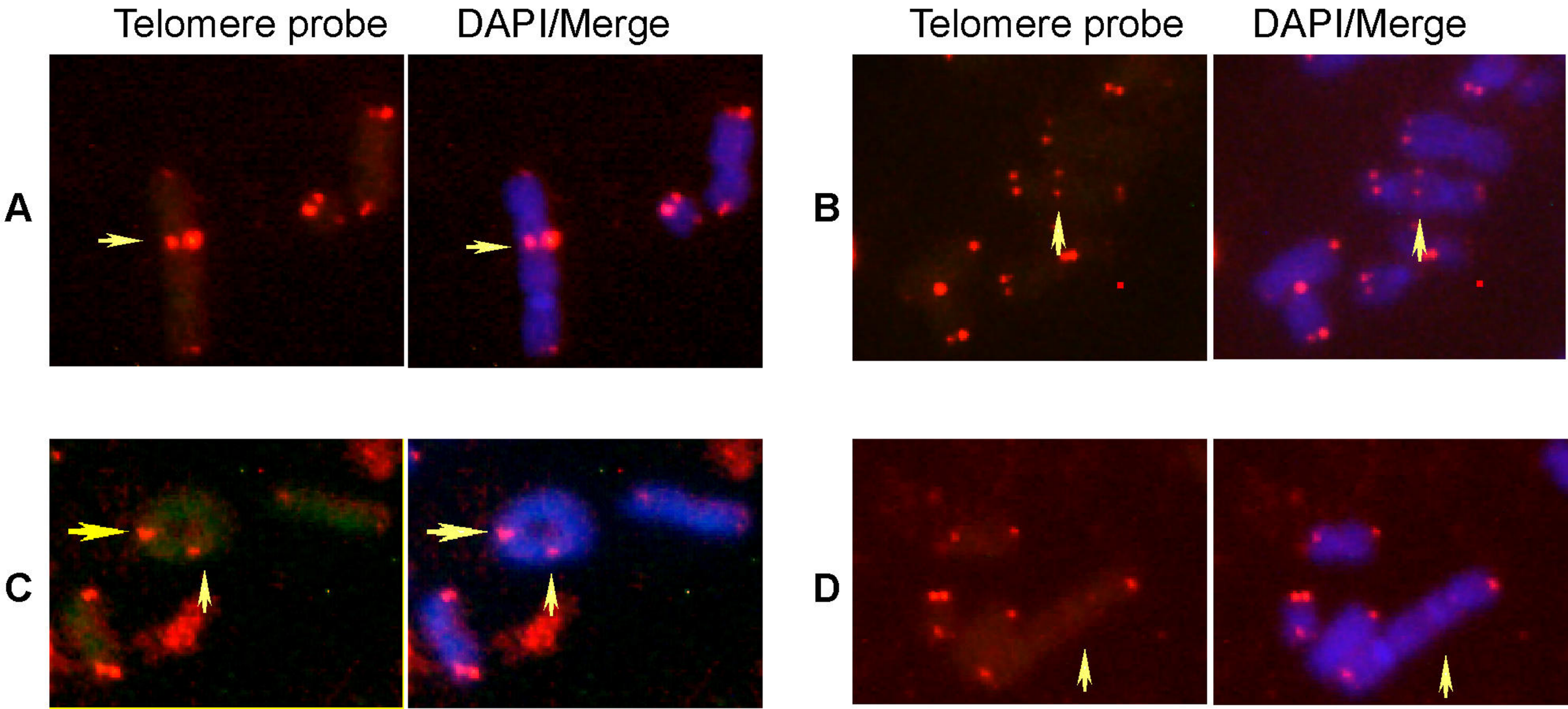

Supplementary Figure 5